Gait Dynamic Stability Analysis with Wearable Assistive Robots

by

Seyed Mostafa Rezayat Sorkhabadi

A Thesis Presented in Partial Fulfillment
of the Requirements for the Degree
Master of Science

Approved June 2018 by the
Graduate Supervisory Committee:

Wenlong Zhang, Chair
Hyunglae Lee
Panagiotis Artemiadis

ARIZONA STATE UNIVERSITY

August 2018

ABSTRACT

Lower-limb wearable assistive robots could alter the users gait kinematics by inputting external power, which can be interpreted as mechanical perturbation to subject normal gait. The change in kinematics may affect the dynamic stability. This work attempts to understand the effects of different physical assistance from these robots on the gait dynamic stability. A knee exoskeleton and ankle assistive device (Robotic Shoe) are developed and used to provide walking assistance. The knee exoskeleton provides personalized knee joint assistive torque during the stance phase. The robotic shoe is a light-weighted mechanism that can store the potential energy at heel strike and release it by using an active locking mechanism at the terminal stance phase to provide push-up ankle torque and assist the toe-off. Lower-limb Kinematic time series data are collected for subjects wearing these devices in the passive and active mode. The changes of kinematics with and without these devices on lower-limb motion are first studied. Orbital stability, as one of the commonly used measure to quantify gait stability through calculating Floquet Multipliers (FM), is employed to asses the effects of these wearable devices on gait stability. It is shown that wearing the passive knee exoskeleton causes less orbitally stable gait for users, while the knee joint active assistance improves the orbital stability compared to passive mode. The robotic shoe only affects the targeted joint (right ankle) kinematics, and wearing the passive mechanism significantly increases the ankle joint FM values, which indicates less walking orbital stability. More analysis is done on a mechanically perturbed walking public data set, to show that orbital stability can quantify the effects of external mechanical perturbation on gait dynamic stability. This method can further be used as a control design tool to ensure gait stability for users of lower-limb assistive devices.

DEDICATION

To my beloved mother, who is the main reason for all I have achieved

And to my newborn niece, Joan, who has brought joy and hope to my family

ACKNOWLEDGMENTS

Contents

List of Figures

Chapter 1

INTRODUCTION

During the past decades, the world is aging drastically. According to the report from U.S. Department of Commerce, the proportion of the people over 65 has been increased to 7% by 2000 and will keep rising to 16% by the end of 2050 (figure 1.1). Aging leads to a challenge of impaired mobility, as around 10 to 20% elderly adults have difficulty, or require external support from another person or device, to walk (Alexander, 1996). Walking is the fundamental component of humans daily life and it significantly influences the quality of ones life. Traditional treatment and rehabilitation technologies are expensive, time-consuming and labor-intensive. In observation of those challenges, technologists and scientists have been actively seeking the development of exoskeletons and orthoses designed to augment human locomotion. Gait wearable sensors and robotics have attracted significant attention, as they provide a personalized system for patients and people with disabilities, to perform rehabilitation training remotely and help them retrieve their capabilities to do their normal daily activities.

Falling is another issue for the elderly and people with disabilities. As people age, the quality of gait becomes less because of negative changes in the neuromusculoskeletal system and the risk of falling increases. A large proportion of falls occurs during locomotion (Berg *et al.*, 1997). It is essential to quantify the risk of falling so it can be detected and prevented. Falling has been correlated with gait instability, but quantifying the gait dynamic stability has still remained controversial. Lower-limb assistive devices can be utilized to ensure more walking stability. However, usually, the application of these devices are more on providing power to help the lower-limb
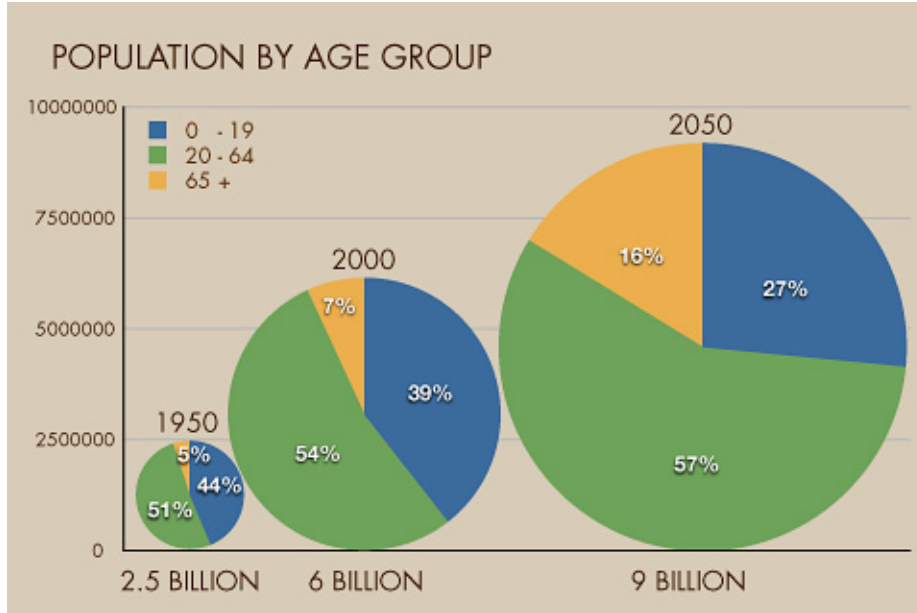
Figure 1.1: World population trend by age group (Perry, 2015)

movement, rather than stabilizing the locomotion. This raises the question of how these wearable robots that are supposed to accompany the elderly and patients in their daily activities, will affect the gait dynamic stability.

The remaining of this chapter will give an overview of gait wearable assistive robots (section 1.1) and dynamic gait stability (section 1.2), and will discuss problem statement (section 1.3) and contribution (section 1.4) of this dissertation.

1.1 Gait Wearable Assistive Robotics

One way to quantify the human gait is to measure the lower-limb joint mobility and the muscle activity during different walking activity. The overall goals for the joint movements and muscle activity are to achieve weight acceptance, single limb support and limb advancement. During stance phase where the foot is in touch with the ground, the weight acceptance and single limb support are the priority tasks. On
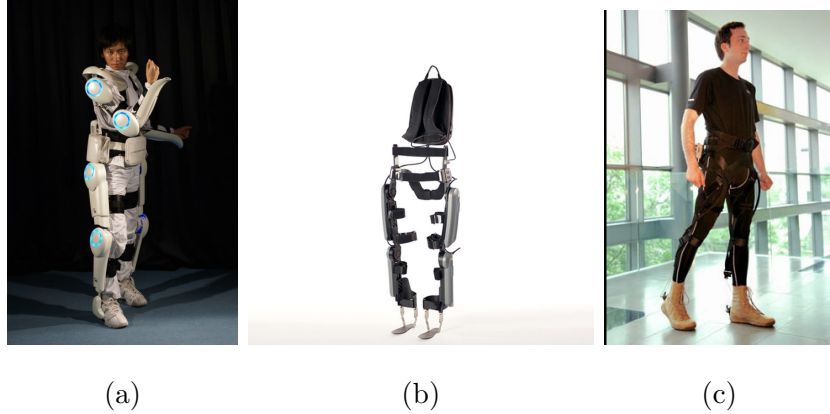
Figure 1.2: Examples of robotic rehabilitation devices: (a) Hybeid Assistive Limb (HAL), (b) Rewalk, (c) Soft Exosuit from Harvard University. (Deng *et al.*, 2018)

the other hand, the limb advancement shifts to the top requirement during the swing phase when the foot is off the ground (Perry *et al.*, 1992). The wearable gait assistive robots are to augment these motions and activities, during normal walking, or to apply walking rehabilitation treatment to patients. Although their application can extend to other daily activities like ascending/descending stairs, sit-to-stand transfer and carrying heavy loads. Exoskeletons and orthoses are defined as mechanical devices that "are worn by an operator and fit closely to the body, and work in concert with the operator's movements" (Herr, 2009). In general, exoskeletons are the devices that augment the performance of the able-bodied user, while orthosis is typically used to describe a device that assists a person with a limb pathology (Herr, 2009).

The gait wearable robots can be classified into two categories: medical and non-medical applications (Vukobratovic *et al.*, 2012). The medical ones are used to provide mobility to physically disabled, injured or weak persons who have walking difficulties. Non-medical ones are used by healthy subjects like soldiers, to perform physically demanding tasks.

The MIT-Skywalker robot is used for rehabilitation treatment of patients with

stroke and nerve injury (Artemiadis and Krebs, 2011). Lokomot is a rehabilitative treadmill-based body weight support device that is powered at the hip and knee (Colombo *et al.*, 2000). The Active Leg Exoskeleton (ALEX) is a powered leg orthosis with linear actuators at the hip and knee joints, and with a force field controller developed to provide assistance to the patient by using the assist-as-needed approach (Banala *et al.*, 2009). The gait rehabilitation robot LOPES (LOwer-extremity Powered ExoSkeleton) can move in parallel with the legs of a person walking on a treadmill (Veneman *et al.*, 2007). The Berkeley Lower Extremity Exoskeleton (BLEEX) was can help soldiers to carry heavy loads, with seven DOF per leg: three DOFs at the hip joint, one DOF at the knee joint, and three DOFs at the ankle joint (Chu *et al.*, 2005; Varol *et al.*, 2010). It was reported that BLEEX wearers can walk at an average speed of 1.3 m/s while carrying a 34 kg payload.

Lower-limb orthoses that are able to help impaired people regain their natural gaits, have gained lots of attention. Ankle-foot orthoses (AFOs) are to control the position and motion of the ankle. AFOs can be used to support weak limbs or to position a limb into a more normal position. AFO's can be classified into 3 categories: fully active, semi-active and passive (Shorter *et al.*, 2013). The Michigan AFO powered by pneumatic actuators uses functional electrical simulation (FES) to control the artificial pneumatic muscles. The device is able to generate the torque for dorsiflexion and plantarflexion motion (Ferris *et al.*, 2005). Both the semi-active and fully active AFOs require at least one sensor to give feedback signal to the control system which helps the device to figure out the user intention (e.g. lifting the toe) and the users assistance requirement. However, semi-active AFO only controls the impedance of the ankle joint in real time. The magneto-rheology (MR) AFO uses MR dampers to generate resistive plantar-flexed torque during swing and initial stance phase (Furusho *et al.*, 2007). Due to the weight and power supply issues, the semi-active and fully

4

active AFOs are not always suitable for a wearable walking assist device. The passive AFO, on the other hand, is commonly used in clinic rehabilitation. The passive AFO can be classified into two categories: articulated, containing an activated ankle joint, and non-articulated device.

1.2 Gait Dynamic Stability

Dynamic Stability is a well-defined concept in mechanics theory, which is the system response to perturbations; If the states of the system stay in a certain range or if they go unbounded. When mechanical system analysis are applied to biomechanics, some hypothesis about the type of system governing gait control is required (Dingwell and Kang, 2007), which are highly non-linear, complex to most extent, unknown. Numerical methods are generally used to quantify the walkings dynamic stability. However no method is commonly accepted (Karčnik, 2004; Dingwell and Kang, 2007) and their relationship to real life notion of stability, which is the risk of falling, is still unclear. Some of these methods are maximum finite time Lyapunov exponents, maximum Floquet multipliers (FM), and gait variability (Karčnik, 2004; Dingwell and Kang, 2007; Bruijn, 2010; Hurmuzlu and Basdogan, 1994).

Gait variability is referred to as the fluctuations of gait parameters over strides. Maximum finite time Lyapunov exponents quantify the systems response to small, or local, perturbations continuously in real time. Floquet multipliers quantify the tendency of the systems state to return to the periodic limit cycle after perturbations.

There has been a widespread effort to evaluate and asses these aforementioned measures of dynamic gait stability. In chapter 4, a more detailed study on these measures are provided and a method is proposed to analyze the gait dynamic stability with wearable assistive devices. Locomotion dynamic stability for biped and humanoid robots have widely been studied (Hürmüzlü and Moskowitz, 1986; Garcia

et al., 1998; Hurmuzlu *et al.*, 2004; Hamed and Gregg, 2017; Hamed and Grizzle, 2014a). However, there has not been much work done on the stability analysis of gait wearable assistive robots, where the robot affects and alters the gait kinetics and kinematics. Barbareschi *et al.* (2015) has studied the kinematics and kinetics changes made by REX Bionics in the rehabilitation process, to human normal gait to evaluate its dynamic stability. Barbareschi *et al.* (2015) has reported that the overground robotic walking training with the i-Walker has improved the gait stability be reducing the number of falls.

1.3 Problem Statement and Motivation

The goal of this dissertation is to perform an analysis on gait dynamic stability with two wearable robots: a knee exoskeletons that provides personalized assistive torque to knee joint during the stance phase using an automatic impedance tuning algorithm, and the robotic shoe, which provides ankle push-up torque to assist the toe-off gait phase.

The assistive power from these exoskeletons are basically external perturbations to the gait, and potentially alter gait kinetics, kinematics, and consequently, its dynamic stability. Tej Chinimilli *et al.* (2018) reported that assistance from the knee exoskeleton has reduced the participants knee range of motion and step length but increased walking cadence.

Thus, the kinematic changes caused by these devices needs to be studied, and introducing and performing a analysis to quantify the gait stability with those devices is essential, which also can be considered as a control design tool for lower-limb assistive and rehabilitative devices.

1.4   Contribution of the Work

- Contributing to the design, control, experimental setup and data collection for two gaits wearable assistive device (chapter 2)

- Analyzing the lower-limb joint kinematics for different modes of assistance with the two wearable devices, and its relationship to gait stability (chapter 3)

- Proposing the orbital stability as an appropriate measure to quantify gait stability with assistive robots (Chapter 4)

- Performing non-linear time series analysis on gait kinematic data to derive the the Floqute Multipliers to quantify and compare orbital stability analysis for the two assistive devices in different modes (Chapter 4)

- Performing orbital stability analysis on a public dataset of perturbed walking to quantify the effect of perturbations on gait dynamic stability (Chapter 4)

Chapter 2

AN OVERVIEW OF THE DESIGN, CONTROL, AND PERFORMANCE OF THE KNEE EXOSKELETONS AND THE ROBOTIC SHOE

In this chapter, the mechanical, electrical and control design process of a knee exoskeleton and a robotic shoe has been addressed, by focusing on the contribution of this dissertation on their development. These assistive devices have been successfully tested on human subjects, and shown to be able to assist human by reducing the corresponding muscle activity. The kinematic data of these experiments has been collected, which later on has been analyzed and used to asses how these robotic exoskeletons affect human gait dynamic stability.

In section 2.1 the mechanical characteristics of the knee exoskeleton are described, and its control development is elaborated. Section 2.2 discusses the novelty design of the robotic shoe, along with its hardware and mechatronic design development.

2.1 Knee Exoskeleton

A knee robotic exoskeleton has been designed and manufactured at RISE lab, ASU. It serves as a wearable assistive device to assist human knee joint by providing assistive torque. The torque is provided through a compact rotary series actuator (cRSEA), in which a worm gear and spur gear combination are used to amplify the assistive torque generated by a Maxon RE 40 150W DC Motor, which is used to power the exoskeleton. The cRSEA is compact and light which avoids unbalance and discomfort to users (Kong *et al.*, 2012). The gear set provides a combined reduction ratio of 63.6:1. The maximum velocity on the human side is 120 rpm and the maxi-
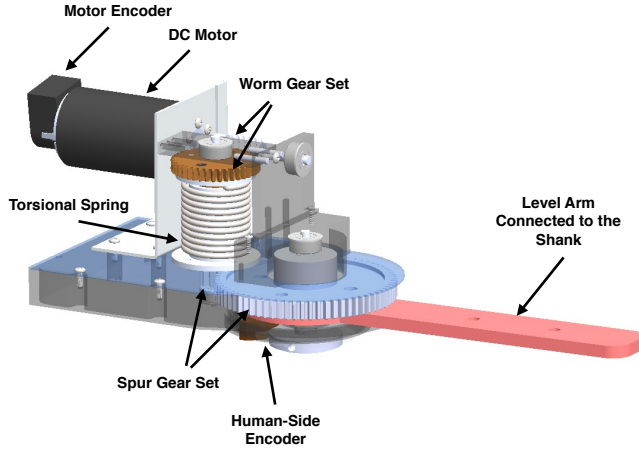
(a) The CAD model and components
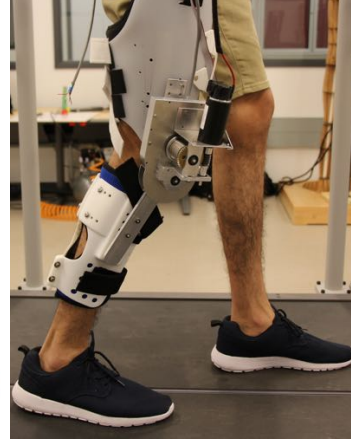
(b) The knee exoskeleton worn by the subject

Figure 2.1: The knee exoskeleton used to provide knee assistive torque

mum torque that the exoskeleton can provide is 11.26 N.m. Two incremental optical rotary encoders are employed to measure motor and human knee angular position. A torsion spring as the elastic element of cRSEA is used which play the role of a torque sensor, as well as an energy buffer to protect the user from unexpected high motor torques. Figure 2.1 shows the CAD model, components and how it is placed on the subject lower limb.

2.1.1 Mechatronics and Control Design

The knee exoskeleton provides assistance using the impedance control law:

$$T_d(t) = k(\theta_h(t) - \theta_0) + b\dot{\theta}_h(t), \tag{2.1}$$

where T_d is the desired torque, k, b, and θ_0 are the actuator stiffness, damping and set point angle, and θ_h is knee angle measurement from human-side encoder. The stiffness, damping and set point angles comes from a personalized automatic impedance tuning (AIT) algorithm based on real-time activity recognition and gait phase detec-

tion (Tej Chinimilli *et al.*, 2018).

Regarding the rotary series elastic structure of the KAD, the torque is generated by the deflections of two sides of the torsional spring which is also amplified by the spur gear set:

$$T = K_s(\theta_{M*} - \theta_{h*})N_s, \tag{2.2}$$

$$\theta_{H*} = \frac{\theta_h}{N_S} \tag{2.3}$$

$$\theta_{M*} = \theta_M \cdot N_W \tag{2.4}$$

where T is the torque provided by the KAD, θ_M is the motor angle, N_s and N_W are the spur and worm gear ratios, θ_{M*} and θ_{h*} are the worm and spur gear angles. Hence, the position reference for the motor can be calculated using (2.2) to (2.4), and the desired torque given by (2.1), and the torque control problem is converted to a position control problem of the motor. To have the motor tracks the desired
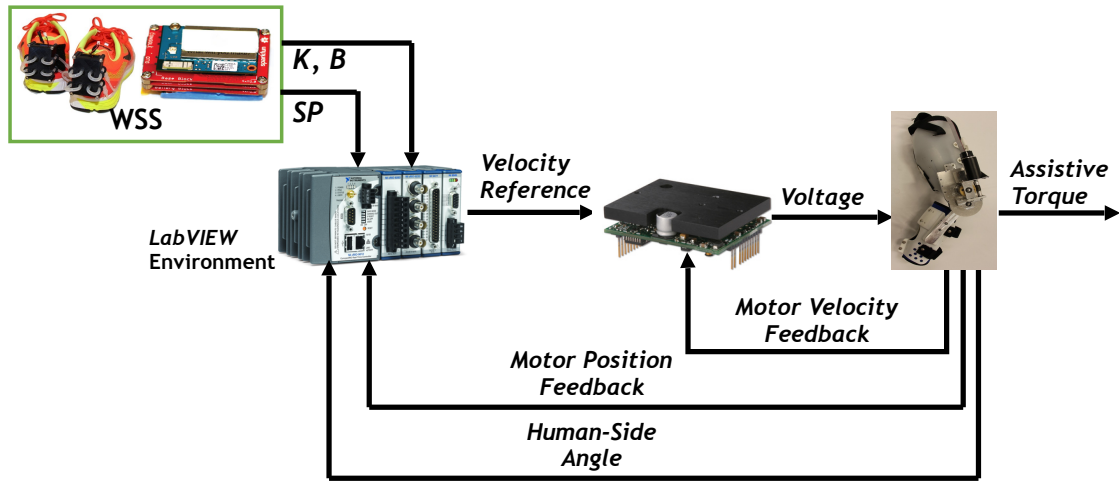
Figure 2.2: The control structure for the knee exoskeleton. WSS: wearable sensing system (smart shoes and IMUs), SP: setpoint knee angle condition, K: actuator stiffness value, B: actuator damping value.

position, a mechatronic setup has been established that is shown in figure 2.2. The wearable sensing system consists of smart shoes and IMUs. Smart shoes measure ground contact forces (Chinimilli *et al.*, 2016), and along with IMUs measurement, are used to provide real-time activity recognition and gait phase detection (Chinimilli *et al.*, 2017). A cascaded PID (proportional-integral-derivative) control structure is used to control the motor angular velocity. This control strategy is implemented using the NI cRIO-9074 as the controller and the AMC DZRALTE-025L200 motor driver. The NI cRIO is programmed through LabVIEW. The inputs to the cRIO are K, B, and setpoint angle from the wearable sensing system and AIT algorithm, human sidearm (knee) angle, and motor angle as the feedback of the control loop. cRIO calculates the position reference from these inputs in real time, and using the motor position as the feedback, shapes a control loop (outer loop) with a proportional control law to provide the velocity set-point to the motor driver. The motor driver uses the motor velocity as the feedback and controls the velocity of the motor using a PID controller (inner loop).

It has been shown by (Tej Chinimilli *et al.*, 2018) that the knee exoskeleton was able to reduce the RMS value of EMG signal of Vastus Medialis of two subjects; reducing the corresponding muscle activity, by providing assistive torque in the stance phase.

2.2 Robotic Shoe

The robotic shoe is a light-weighted wearable gait assistive device, designed and fabricated at ASU RISE lab, to provide dorsiflexion assistive ankle torque, at toe-off gait phase. A linear spring is used in the mechanism to store the energy at heel strike, a ratchet-pawl locking mechanism to lock the spring and releasing it at terminal stance to assist the toe-off.
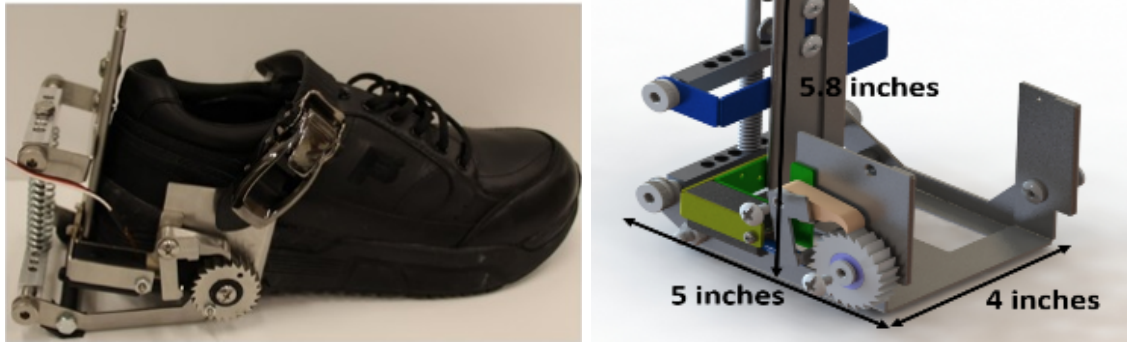
(a) The complete mechanism with the shoe   (b) The CAD model with frame dimensions

Figure 2.3: The robotic shoe mechanism

2.2.1 Frame Design

The frame is designed so that it can fit in the back of a regular size 12 shoe. The spring is placed such that it will store the energy at the heel strike, which is exerted by human weight, and provide dorsiflexion torque in heel-off to toe-off. A compression spring is chosen such that it can easily be compressed at heel strike, with the maximum load of 134 N, to partially support the push-up ankle torque needed. It was attempted to keep the frame as light and compact as possible, so the added inertia would not be significant. Figure 2.3 shows the frame design and how it is mounted on the shoe.

2.2.2 Locking Mechanism and Actuation System

It is important that the stored potential energy by the spring at the heel strike, be released right before toe-off, so it can effectively provide a push-up ankle torque. Therefore the spring displacement needs to be locked after it is fully compressed, and then gets unlocked right before the toe-off stage, or at terminal stance. If the spring

just gets compressed and released by itself (passive mechanism), some part of the energy will be wasted and not only will not help the toe-off, but also will perturb the normal gait cycle and affect the gait stability, as it will exert push-up force before the heel-off, especially in slow walking that the duration between the heel strike and toe-off is considerable.

A locking mechanism that utilizes a ratchet-pawl system is used, Figure 2.4 shows how this mechanism works. While the subjects heel is touching the ground, the spring is compressed and the ratchet rotates in a clockwise direction. After the heel strike phase, the pawl will stop ratchet from rotating in a counter-clockwise direction which in serial, locks the spring in its maximum deflection and restores the energy within the spring. During the toe-off phase, the pawl is lifted by an actuator and release the energy to assist the toe-off motion. To lift the pawl and unlock the mechanism

Step 1: Initial Position grey frame is connected to the shoe fixed with a ratchet belt

Step 2: compress the spring during heel-strike phase

Step 3: lifting the pawl by extruding the blue linear actuator rod

Step 4: lifting the grey frame by fixing the lemon bottom part to the ground
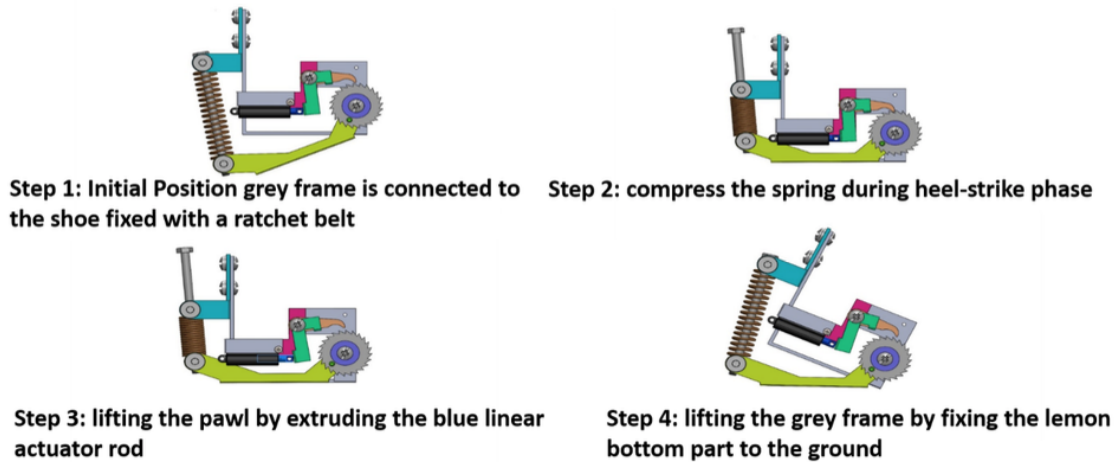
Figure 2.4: The locking mechanism used in the robotic shoe to store and release the energy

when the spring is fully compressed, a torque of 0.367 N.m is required, measured using a force gauge. The PQ12 linear actuator is used to lift the pawl and unlock the mechanism, with help of a lever arm. This actuator is very light (15g), and is able to

exert the required force (16 N).

It is also needed to identify the terminal stance gait phase, so the actuator unlocks

| (a) Spring locked | (b) Spring unlocked |

Figure 2.5: The robotic shoe in action: (a) shows the instance that the spring is compressed and locked by the ratchet-pawl mechanism (midstance). (b) shows the beginning of toe-off when the spring is released by the actuator and is exerting push-up force.

the spring at that instant. Therefore a force sensor (Flexiforce A401) is mounted at the bottom of the shoe. With the help of its measurement, the terminal stance gait event can be identified in real time. An Arduino Nano ATmega328 serves as the micro-controller, which reads the force sensor and command the actuator to release the spring when the measurements exceed the threshold, which is specified based on each user ground contact forces. Figure 2.5 shows a subject walking on the treadmill wearing the robotic shoe in active mode.

2.3   Summary

This chapter discussed the design and control of two lower-limb assistive devices: The knee exoskeleton and the robotic shoe. The knee exoskeleton uses a cRSEA mechanism to provide personalized knee assistive torque in stance phase using the

AIT algorithm, and a cascaded PID technique to control the motor position. It has been shown to decrease the targeted muscle activity. The robotic shoe is a light-weighted mechanism that provides ankle dorsiflexion torque to assist the toe-off gait phase, using a spring and and an active locking mechanism.

In the next chapter, the kinematic data collected wearing these robots will be presented and studied to see how it alter human gait kinematics, and obtain insight on their effects on gait dynamic stability.

Chapter 3

GAIT KINEMATIC ANALYSIS WITH WEARABLE ASSISTIVE ROBOTS

In this chapter, the lower-limb joint kinematics of subjects walking with and without the two wearable assistive robotics has been represented. The study has been done for both robotic shoe and the knee exoskeleton, on two participants, in three modes: Normal walking (without the wearable robotics), wearing the devices in passive mode and wearing the devices in active mode. The lower-limb joint motions have been collected in a motion capture laboratory using high-speed infrared cameras and instrumented treadmill.

The purpose of this chapter is to exhibit how these wearable robots alter gait kinematics. Changing the gait patterns can affect the gait stability. Gait variability has been one of the measures to analyze and quantify gait stability. Therefore besides lower-limb joint angular motions, their deviation from the steady state walking pattern has been presented which can give a better clue to drive the conclusion that gait stability has been affected by the wearable robots.

In the following, first the data collection and processing procedure is described in section 3.1. The results for the exoskeletons and robotic shoe are presented in sections 3.2 and 3.3, respectively. Section 3.4 discusses the results and the conclusions that can be drawn.

3.1 Data Collection and Processing

To obtain the gait kinematics, it is needed to collect the lower-limb motion data multiple strides. Each experiment was set up in the motion capture laboratory at Polytechnic campus, Arizona State University (ASU), and was approved by the Insti-
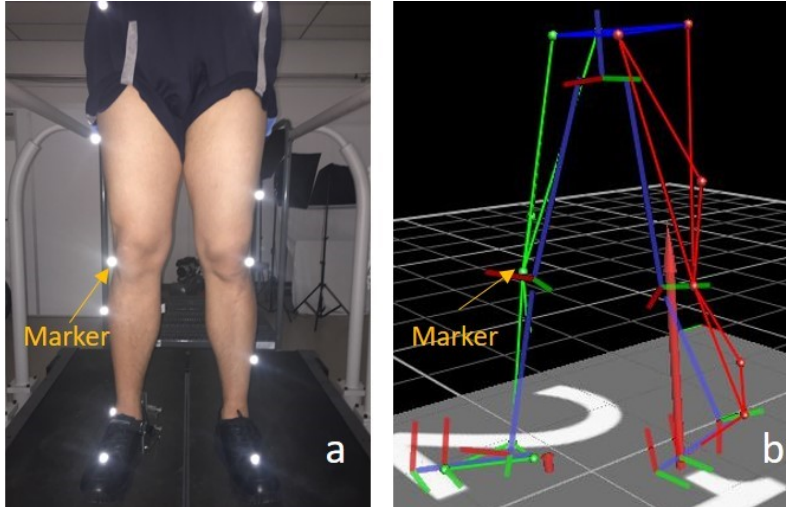
Figure 3.1: Recording lower-limb motion: (a) Marker placement on the subject, (b) the lower-limb skeleton model built in Vicon software environment

tutional Review Board (IRB) at ASU (STUDY00007601). The laboratory is equipped with 12 high-speed infrared cameras (Vicon Motion Systems Ltd.,) and instrumented treadmill (Bertec Corporation). In each experiment, 16 markers were mounted at specific positions on the participants to capture the lower-body motion with the frame rate of 100 Hz. With help of these markers, the lower-limb skeleton model was built and hip, knee, and ankle angular motions were extracted, using Vicon plugged-in gait model (figure 3.1). Each participant walked on a treadmill for at least 2 minutes for each trial. The participants information are represented on table 3.1.

To study gait kinematics, each joint angular motion is presented as the average of the whole strides, along with the 97.5% interval confidence, in a gait cycle. Gait cycles are defined from heel strike to the next heel strike. Figure 3.2 shows the gait phases.

Table 3.1: Participants information in each experiment

Experiment	ID	Gender	Weight (kg)	Height (cm)
Knee Exoskeleton	1	Male	60	180
	2	Male	78	183
Robotic Shoe	1	Male	77	183
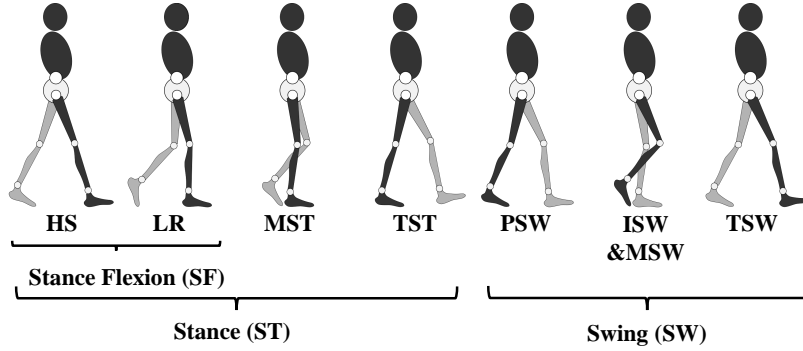
Figure 3.2: The gait cycle of human walking. HS - heel strike, LR - loading response, MST - mid stance, TST - terminal stance, PSW - pre-swing, ISW - initial swing, MSW - mid-swing, and TSW - terminal swing. (Tej Chinimilli *et al.*, 2018)

3.2   Gait Kinematics with the Knee Exoskeleton

The experiments for subjects with knee exoskeleton includes three trials: Subject normal walking (without the exoskeleton), subject wearing the exoskeleton in passive mode; meaning no assistance is provided by the exoskeleton and the subject drives it, and subject wearing the exoskeleton in active mode; meaning active assistive torque is exerted by the exoskeleton.

Figure 3.3 clearly show that joint kinematics of the right leg is significantly affected by wearing the exoskeleton in passive mode. The knee range of motion has decreased, along with its variability, which is reasonable since the exoskeleton makes the knee motion restricted. On the other hand, the variability of the left knee in passive mode
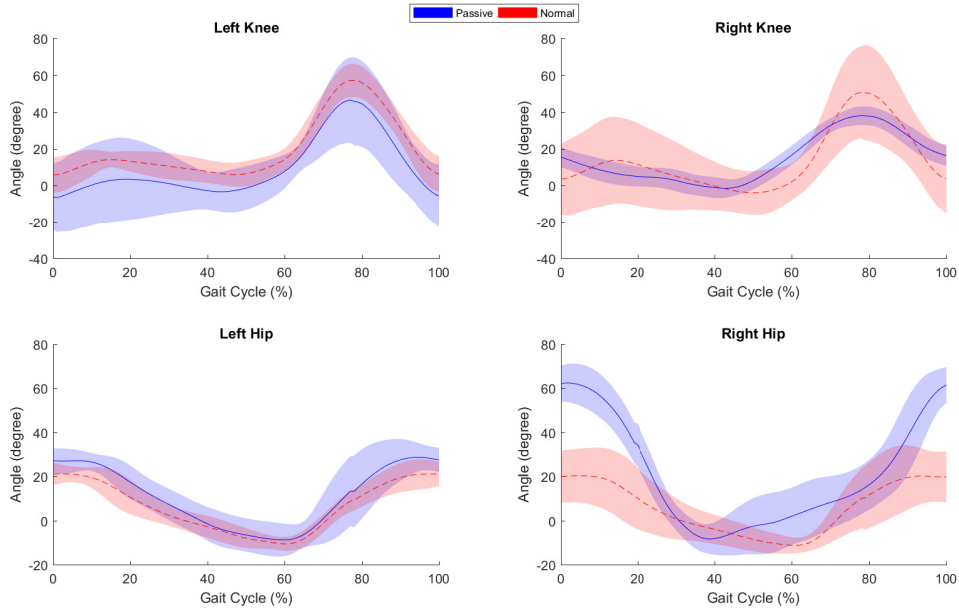
Figure 3.3: Hip and knee average and 3σ (shaded) sagittal plane joint angles for subject 1 in the passive and normal mode with the knee exoskeleton.

has significantly increased, which can be explained by the fact that left knee makes up for the restricted motion of the right knee in passive mode. The right hip motion in passive mode is remarkably different from its natural motion. The subject's hip extension in passive mode has increased, most probably because the subject had to extend his right hip more to compensate the restricted knee motion, so the whole leg motion can keep its natural walking pattern.

To observe the effects of assistance from the knee exoskeleton, figure 3.4 compares the active and passive mode joint kinematics. The right leg knee range of motion is higher and closer to its normal walking in active mode compared to passive mode, meaning the assistive torque is helping the subject to extend more his knee in the sagittal plane. Also, it is causing the right hip range of motion to get back to its natural amount. The motion variability of the left knee, hip, and right hip are less in
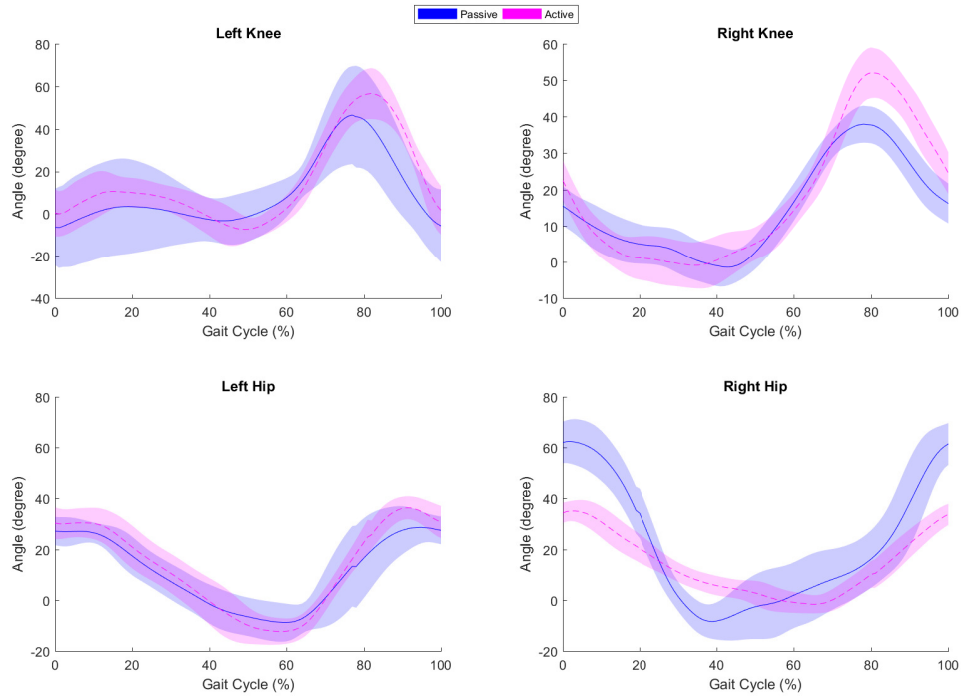
Figure 3.4: Hip and knee average and 3σ (shaded) sagittal plane joint angles for subject 1 in the passive and active mode with the knee exoskeleton.

active mode and more comparable to the normal walking. In overall, by comparing figures 3.3 and 3.4, it is clear that the joint motions are closer to the natural walking in active mode, meaning the assistance is causing the subject to retrieve its natural walking, which was significantly affected by wearing the exoskeleton in passive mode.

3.3 Robotic Shoe

Same as the knee exoskeletons, each experiment with the robotic shoe contains three trials: Normal walking without the device, wearing the device in passive and active. The passive mode in the robotic shoe is different from the exoskeleton, in the sense that there is still assistance, however, there is no external power to the mechanism. In active mode, the assistance is timely controlled by the linear actuator.
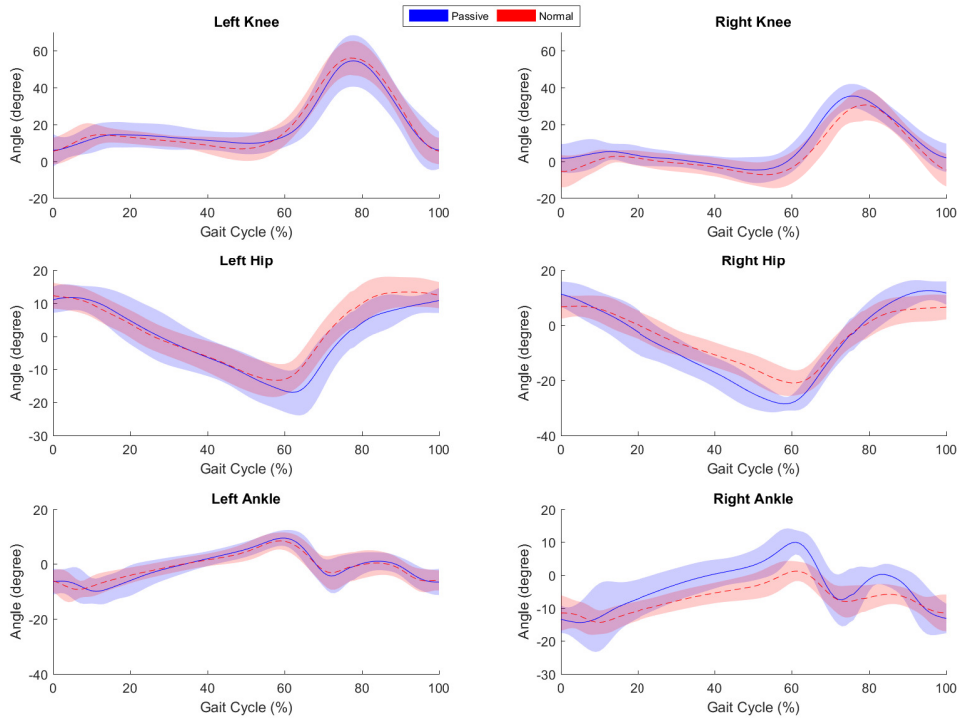
Figure 3.5: Hip, knee, and ankle average and 3σ (shaded) sagital plane joint angles for subject 1 in normal and passive mode with the robotic shoe.

Now it is desired to see how first: the external push-up torque from robotic shoe alter the lower-limb joints gait patterns, and secondly, how actively controlling the push-up torque and exerting it at the right time, will affect the gait kinematics.

Figure 3.5 shows that the joint angles of the right leg, which is the leg that robotic shoe has been put on, are more affected than the other leg. Most importantly, the ankle gait pattern in passive mode is different from the normal pattern. There are two possible reasons to explain the right ankle gait pattern: first the push-up force exerted by the spring, which has caused the increased extension in the stance and toe-off stage, and second, the extended length of the shoe because of the robotic shoe
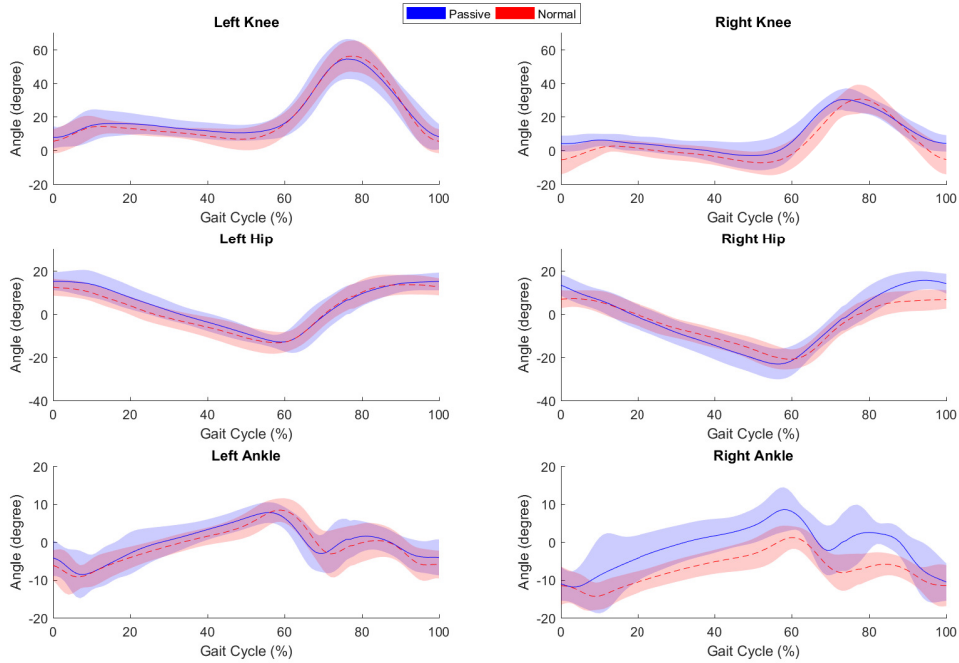
Figure 3.6: Hip, knee, and ankle average and 3σ (shaded) sagital plane joint angles for subject 1 in normal and active mode with the robotic shoe.

mechanism, would cause the user to slightly changes the ankle angle during the swing and heel strike. By comparing the gait kinematics in active mode with normal mode (figure 3.6), it is observed that active mode also has significant effects on ankle joint gait cycle pattern, somehow similar to the passive mode. The peak angle in toe-off is higher than the other two modes, as well as the variability throughout the gait cycle. The other joint gait cycle pattern is just slightly different from the normal pattern, without significant changes in motion variability.

3.4   Conclusion and Discussion

In this chapter, the lower-limb joint kinematics in the sagittal plane (extension-flexion) has been studied. It was attempted to observe how the two wearable assistive

Table 3.2: The mean standard deviation across the gait cycle for lower-limb joint motions with the knee exoskeleton in the three modes of experiment

Mode	Lknee (°)	Rknee (°)	Lhip (°)	Rhip (°)
Normal	7.4	10.9	5.1	10.12
Passive	16.72	5.3	8.2	10.7
Active	8.5	5.9	6.4	4.7

robots affect and alter the gait kinematics, which gives us a better clue toward the stability analysis with these devices. The results with the knee exoskeleton show that wearing the exoskeleton decreases the targeted leg knee range of motion, and slightly changes the pattern. These two changes are more obvious when subject wearing the exoskeleton with no active power and it is driven by the user (passive mode). The hip joint motion of the leg with the exoskeleton also gets remarkably affected in the passive mode, while the active assistance seems to help the subject retrieve its natural gait pattern. The variability of motion for both knees and hip is different in the three modes. Table 3.2 shows the mean standard deviation of joint angular motions from the average pattern. Variability has been referred to as one of the measures to analyze gait stability and risk of falling, and these results lead us to a more comprehensive gait stability analysis with these wearable assistive robots. For the robotic shoe, a significant change was observed in the ankle gait pattern for the leg that the wearable robot was worn, in both passive and active mode. The other leg joints angles were not notably different from the normal pattern, and gait motion variability was not as affected as the one with the knee exoskeleton, although slightly higher than the normal gait cycle.

The knee exoskeleton has significantly affected not only the targeted joint but also

other lower-limb kinematics, as there are kinetic and kinematic inner-coordination between lower-limb joints during the gait. The robotic shoe mostly just alter the targeted joint (ankle) kinematics, as the provided assistance is not as large and comparable to the knee exoskeleton. In the next chapter, it is desired to find out how these kinematic changes can potentially alter the gait dynamic stability.

Chapter 4

DYNAMIC STABILITY ANALYSIS

Providing a stable gait in the sense that it keeps people away from falling and helps them to resist perturbations can be an important feature for lower-limb assistive devices. Significant proportion of falls occur during gait and it poses a major threat for elderly people (Fuller, 2000) and people with gait disabilities (Richardson and Hurvitz, 1995). To asses how those assistive devices affect gait stability, first we need to define an appropriate measures for quantifying dynamic stability during gait cycles.

In theory, stability is a well-defined concept, which relates to the way a system behaves following a perturbation, which should not cause an unbounded change in states variables. Therefore, for the steady state walking to be stable, the state of the system should stay within a certain operating range.

Many walking stability criteria have been proposed, although still no commonly accepted way to define, or quantify, locomotor stability (Karčnik, 2004; Dingwell and Kang, 2007). Measures that are supposed to assess gait stability often reflect a combination of performance and robustness of gait (Bruijn, 2010). Robustness is related to one's ability to handle large perturbations and performance is related to how quick one can handle perturbations and gets back to the safe range. These measures can be helpful in assessing the likelihood of falling. Consequently, we define gait dynamic stability as the ability to respond to perturbations, which can be reflected in those measures.

As the equations of human motion are unknown, numerical methods are used to quantify the walking's dynamic stability. Some of these commonly used meth-

ods, which are derived from dynamical systems theory, are: maximum finite time Lyapunov exponents, maximum Floquet Multipliers (FM), and variability (Karčnik, 2004; Dingwell and Kang, 2007; Bruijn, 2010; Hurmuzlu and Basdogan, 1994). These measures are calculated from time-series data of steady-state walking pattern without any external perturbations. In the following sections, first those measures will be analyzed and then, we explain why orbital stability is chosen to assess the gait dynamic stability for subjects wearing assitive devices. The second section will be on explaining the nonlinear time series analysis and numerical procedure to find FM values for different gait data. The results and final discussion are given on the third and forth sections, respectively.

4.1   Commonly Used Measures to Analyze Gait Stability

Variability: Gait variability is the amount of fluctuation of a certain parameter over strides during walking. some examples including stride time and stride width variability, or variance, the standard deviation or the coefficient of variation of the joint angles (Bruijn, 2010). It has been shown that Increased variability during walking is related to increased risk of falls in the elderly (Maki, 1997). However, it is not correlated with measures of local dynamic stability and can not quantify how the gait responds to perturbations (Dingwell and Cusumano, 2000). Therefore, high variability does not necessarily lead to instability (Brach *et al.*, 2007).

Maximum finite time Lyapunov exponents: Its a measure of local dynamic stability and has been used widely to quantify dynamic stability of gait. They can be a representative of the system's response to small, or local, perturbations continuously in real time. Such perturbations may be present in human gait due to internal (e.g. sensory-motor noise) or external sources. Basically the idea is to find

the distance between the states of the system in time, and see if it is increasing exponentially (unstable) or decreasing (stable). The maximum finite time Lyapunov exponent quantifies the average logarithmic rate of divergence.

This method first was used by Dingwell *et al.* (2000) to quantify dynamic gait stability and since then has become very popular in such studies (Bruijn, 2010). Dingwell *et al.* (2000); Dingwell and Marin (2006); Dingwell *et al.* (2001) have Shown that lower walking speeds leads to more local stability, and that overground walking is less locally stable compared to motorized treadmill.

However, among these findings, it has been reported that all subjects exhibited a some degree of local instability during normal walking, without any fall or stumble. Dingwell and Kang (2007) has mentioned biological noise and small corrections made by the neuromuscular control system to maintain balance, as the main reasons for local instability observed in the gait.

Orbital stability: It is defined for a limit cycle system as the tendency of the system's state to return to the periodic limit cycle after perturbations, and is quantified through Floquet Multipliers (Nayfeh and Balachandran, 2008) for one discrete cycle to the next. Floqquet multipliers (FM) are the rate of convergence/divergence towards a fixed point or cycle, which are the eigenvalues of the linearization (or Jacobian) of the cycle-to-cycle function.

To use this criteria to evaluate the gait's dynamic stability, first we need to assume that gait is a periodic motion, although it actually shows some degree of aperiodic behaviour (Hausdorff *et al.*, 1995). This method were first used in robotic gait to assess the stability of bipedal locomotion (Hürmüzlü and Moskowitz, 1986). It has been less in use for human experiment data compared to local stability method, however it has been found that human walking is orbitally stable (Hurmuzlu and Basdogan, 1994), and postpolio patients were less stable than healthy subjects. Dingwell and Kang

(2007) has also shown that FM values are higher for overground walking compared to motorized treadmill, which agrees with local stability results. McAndrew *et al.* (2011) has reported that both Floquet multipliers and short-term local divergence exponents increase for subjects walking with continuous pseudo-random oscillations in either the visual scene or support surface, while long-term local divergence exponents decrease.

4.1.1   Summary and Discusion

In this study, we want to see how wearing our knee and ankle assistive devices affect human gait dynamic stability. As explained in the previous sections, both local stability and orbital stability methods has been widely used to assess human gait dynamic stability. Dingwell and Kang (2007) has shown that normal walking is orbitally stable while it shows some degree of local instability. They suggest that it can be due to different properties of system dynamics, which are reflected in local and orbital stability, as they were not able to find significant correlations between these two measures. In calculating FM values each trajectory is compared to a single reference trajectory while for short and long-term local divergence exponents, each trajectory is compared to its own nearest neighbor, which can be the reason why their results are different. Mathematically, it is possible that a limit cycle shows orbital stability while being locally unstable (Ali and Menzinger, 1999). It has been also reported that adding noise to the the simplest mechanical model of bipedal walking, to make the model walk down an irregular slope, leaded to significant local instability, while being orbitally stable (Garcia *et al.*, 1998). These findings seem to make the orbital stability a more meaningful method for evaluating how assistive devices alter the overall stability of human walking, in the sense of how it responds to perturbations, and real-life notion of stability, which is the risk of falling, as the inertia and torque exerted by these devices are actually some kinds of perturbations to

human neuromuscular system. Orbital stability has been used for controlling bipedal robots to to stabilize their walking pattern (Hurmuzlu *et al.*, 2004; Hamed and Gregg, 2017; Hamed and Grizzle, 2014a). However the author has not found any work on using it for rehabilitation and assistive purpose. One goal of this study is to use its analysis and result to combine with the control of gait assistive and rehabilitative robots in order to make sure patients are following stable trajectories, along with assistance provided to them. Therefore, orbital stability can be a better measure for this application, as normal walking can be sometimes locally unstable, and there are already a reach literature on using orbital stability criteria for controlling and stabilizing purposes of robot locomotion.

4.2   Quantifying Gait Orbital Stability from Kinematic Time Series

To quantify the gait dynamic stability, any kinematic time series can be used. As human walking motion is highly non-linear, non-linear time series analysis techniques are to be used to calculate the Floquet Multipliers.

4.2.1   Nonlinear Time Series Analysis

To extract dynamical information of the kinematic time series, the nonlinear times series analysis methods can be employed, which is build upon chaos and nonlinear dynamics theory.

To study the dynamic behind the gait kinematic time series, we need to construct a corresponding state space. For mechanical systems, these spaces mostly contain positions and velocities of the system's element. However, since the states of walking may be seen as being on an attractor, i.e., "a sub-space of the n-dimensional state space to which neighboring trajectories converge" (Gates and Dingwell, 2009), it has been shown that from one state variable of a system, an attractor can be reconstructed

29

which has the same features as the original attractor with all the state variables. (Takens, 1981).

The procedure to reconstruct the proper state space out of gait kinematic data has been described in details by Dingwell and Cusumano (2000); Hamed and Grizzle (2014b), which is based on standard embedding techniques, and almost all work on gait stability analysis have used this procedure. For each time series data, the state space is constructed from the original state and its time delayed copies:

$$X(t) = [x(t), x(t+T), x(t+2T), ..., x(t+(d_E-1)T)] \tag{4.1}$$

where $X(t)$ is the d_E dimensional state vector, $x(t)$ is the original one-dimensional data, T is the time delay, and d_E is the embedding dimension. The minimum of the average mutual functions has been used to calculate the time delay, which represents "the the amount of information shared between two data sets over a range of time delays", which will provides adjacent delay with a minimum of redundancy (Dingwell and Cusumano, 2000). The embedding dimension can be estimated using a global false nearest neighbour analysis (Kennel *et al.*, 1992), which compares the distances between neighboring trajectories for different successive dimensions. When trajectories that overlap in dimension d_i are distinguished in dimension d_{i+1}, false neighbour occurs.

In this thesis, each lower-limb joint angles are used as the time series data to reconstruct the stat-space and evaluate orbital stability. Both joint angles and trunk accelerations are used for this purpose (Dingwell and Kang, 2007; Bruijn, 2010; Hurmuzlu and Basdogan, 1994), however in order to observe the effects of assistive robots on each individual joint motion stability, the state spaces are constructed from each joint kinematics. By employing this technique, a more detailed analysis can be done on the effects of the assistive device on gait dynamic stability. It should be also noted

that lower-limb joint angles are usually measured and used as feedback by assistive devices, therefore they can be used to control the gait dynamic stability by the assistive robots. Each joint motion might be affected in a different way and based on that, they can be targeted by the assistive device to improve the gait stability.

4.2.2   Calculating FM

Orbital stability can be quantified through FM values based on standard techniques (Hurmuzlu and Basdogan, 1994; Hürmüzlü and Moskowitz, 1986) which has been used widely for orbital stability analysis of gait (Dingwell and Kang, 2007; Bruijn, 2010; Nayfeh and Balachandran, 2008; McAndrew *et al.*, 2011).

In Floquet theory, it is assumed that a system is strictly periodic, therefore the data needs to be time normalized. Then, the state of the system after on cycle is assumed to be a function of its current state:

$$S_{k+1} = F(S_k) \tag{4.2}$$

From (4.2), Poincare sections can be defined for each points of the limit cycle as the orthogonal plane to the flow direction of the limit cycle which it transects all of the limit cycle trajectories.

For the fixed point, average trajectory of the steady state walking is used, which is a reasonable assumption since steady state walking is stable. Small perturbations will cause each trajectory to be deviated from fixed point, and orbital stability can be estimated by using linearized form of (4.2) for each poincare section:

$$S_{k+1} - S^* = J(S^*)(S_k - S^*) \tag{4.3}$$

where S^* is the fixed point and $J(S^*)$ is the system Jacobian at each poincare section. FM values are the eigenvalue of the Jacobian which exhibit the rate by which small

perturbations grow or decay. Therefor, for limit cycle to be orbitally stable, these FM must be inside unity circle (i.e., $|FM| < 1$). For each poincare section, FM are calculated and the max FM will be be reported as it shows the most instability for each poincare section. Figure 4.4 shows the graphical representation of poincare sections and orbital stability for attractors.
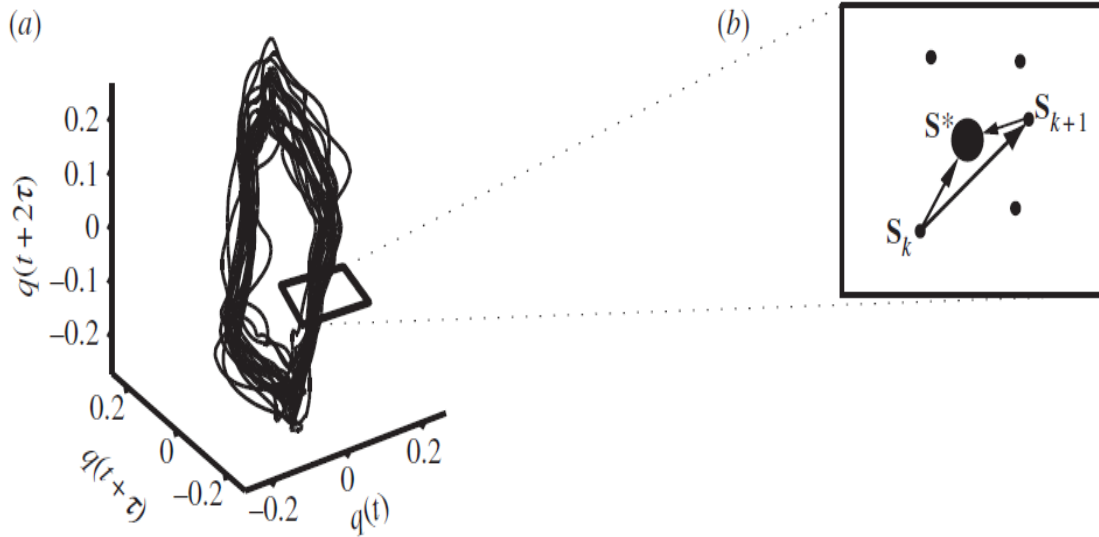
Figure 4.1: Calculation of the maximum Floquet Multipliers. a) The three dimensional attractor (state space reconstruction of q). b) Close-up of the poincare section. The Jacobian maps the S_k to S_{k+1} with respect to $J(S^*)$ which is the average points of all data in poincare section. (Bruijn, 2010)

4.2.3 Numerical Procedure

All the calculation has been done using MATLAB. For each kinematic time series, the following procedure has been followed:

Finding Time Delays

The time delay for constructing time series copies are calculated by finding the first minimum of the average mutual information (AVI), using the MATLAB code provide by Chelidze (2015). The AVI graph for one of the subject's knee joint angle is shown in figure 4.2. For each kinematic time series, corresponding time delay is calculated and used to construct the state space. Usually the time delays were between 15 to 40 samples.
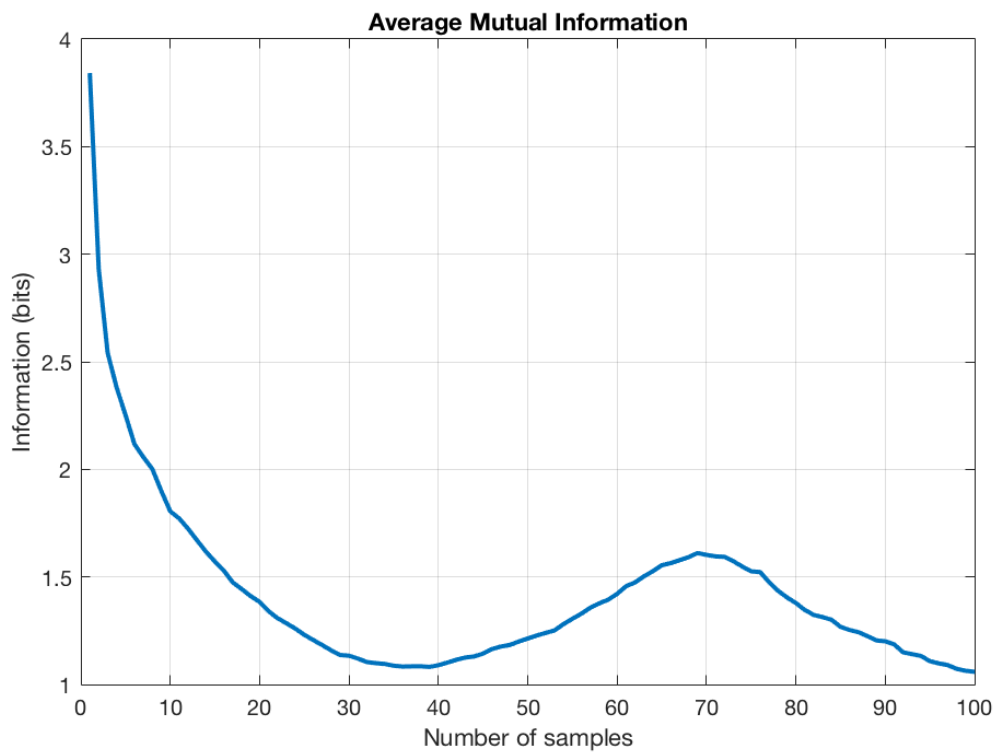
Figure 4.2: The average mutual information calculated for knee joint angle time series of one of the subjects normal walking data. The first minimum happens at T=35, which is used as the time delay to reconstruct the delay coordinated state space

Finding the Embedding Dimension

The embedding dimension was calculated using Global False Nearest Neighbour analysis. For all data, an embedding dimension of $d_E = 5$ seemed appropriate, as for all of them FNNs percentage were close to zero for $d_E > 4$ (figure 4.3). Also in most studies $d_E = 5$ was used to analyze gait data (Dingwell and Kang, 2007; Dingwell and Cusumano, 2000; England and Granata, 2007).
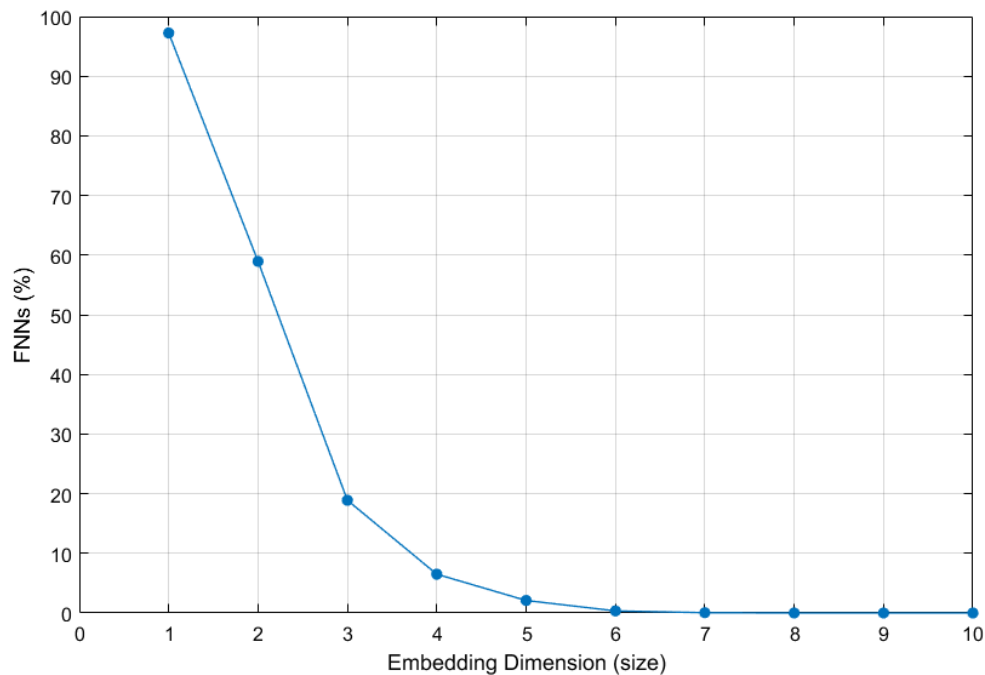
Figure 4.3: The global false nearest neighbourhood percentage calculated for knee joint angle time series of one of the subjects normal walking data.

Reconstructing the State Space

After calculating the time delay and the embedding dimension, a state space is constructed for each time series data, based on (4.1). In order to be consistent for all data and subjects, for each trial that its data been used in this study, the maximum

knee flexion angle is used as the beginning of the each gait cycle, which is when mid swing starts. Usually heel strike is used in most studies of the gait as the beginning of the cycle, however, in some data where subjects had worn knee exoskeleton, the identification of heel strike could be inaccurate because of the alternation of the gait pattern. Figure 4.4 shows the three dimensional state space constructed from one of the joint angles time series data and its delayed copies.
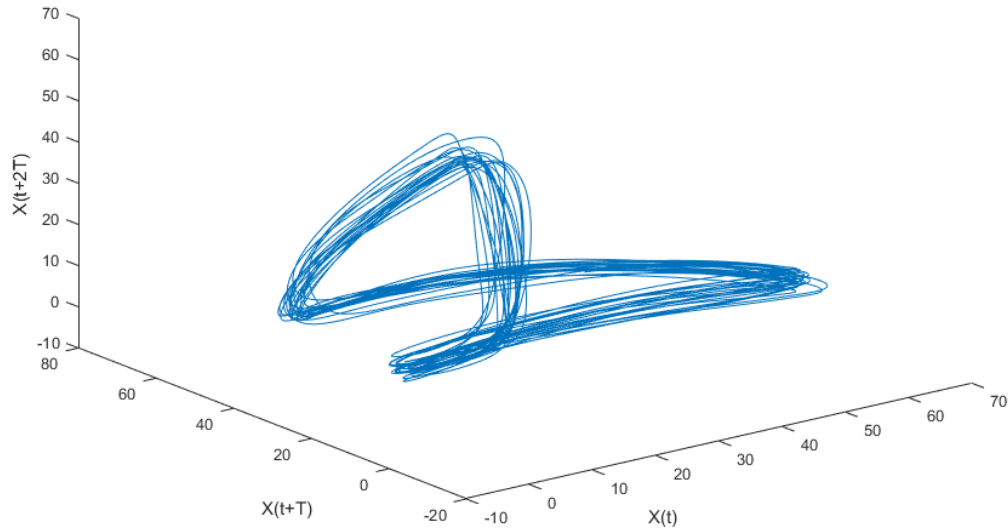
Figure 4.4: the 3-dimensional state space constructed from knee joint angle time series of one of the subjects normal walking data. It clearly show the characteristics of an attractor.

Finding FM values

To use orbital stability criteria, the data needs to be time normalized. Therefore, each gait cycle is normalized to 101 points (from 0 to 100%). Thus, there will be

101 poincare sections that for each, a Jacobian matrix needs to be calculated from (4.3). It is necessary to take an equal number of strides for all data in order to be able to compare the results with each other, since the number of strides taken into consideration will affect the FM values (Bruijn *et al.*, 2009). In this section, 20 strides for each gait data is used to calculate the FM values, which its average should be good enough to get the steady-state gait pattern as the fixed points used in each poincare section. Therefore, for each time series data (which here are joint angles), we will have a three dimensional array of 101 (number of points in each stride) by 5 (embedding dimension, time delayed copies)) by 20 (number of strides).

For each poincare section, the corresponding Jacobian is constructed using the least-square method. The FM values are the magnitude of the eigenvalues of the Jacobian, which only the maximum of them is reported for each poincare section.

4.3   Gait Orbital Stability Analysis Results

In this section, the orbital stability results are presented for normal walking, walking with the knee exoskeleton, walking with robotic shoe, and mechanically perturbed walking.

4.3.1   Normal Walking

Before performing orbital stability analysis on subjects wearing the exoskeletons, first we performed it on three subject normal walking, to evaluate our analysis and compare the results with what is in literature.
The Analysis has been done on three healthy subjects walking on a treadmill with the speed of 0.8 m/s, where their lower-limb kinematics data has been collected the same way described in chapter 3, in a motion capture laboratory. Knee and hip joint flexion/extension motions are considered to perform the analysis, as they are the

36

motions that can be targeted by gait assistive robots. The FM values across the gait cycle for all three subjects are shown in figure 4.5.
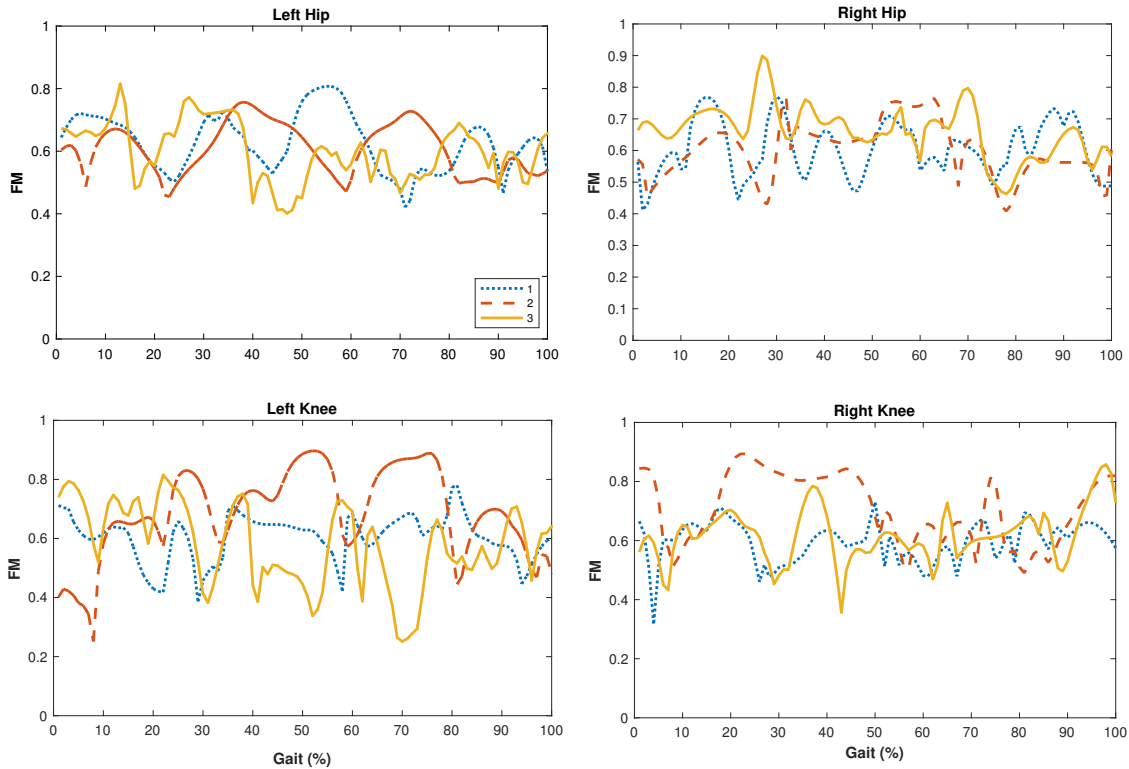
Figure 4.5: Knee and hip joints orbital stability analysis of three healthy subjects normal walking on treadmill with the speed of 0.8 m/s

Based on the results of this section, all subjects are orbitally stable, as non of the subjects knee and hip max FM values exceed one. As it can be seen in the figure 4.5, there is no obvious pattern in the FM values throughout the gait phases. Dingwell and Kang (2007) also reported that they were not able to find any statistically significant relations for how FM values changes across the gait phases. However, the FM plots have somehow similar magnitude and deviations for all three subjects, except for a couple of knee FM values of subject no. 3 (figures 4.5), which they are a bit unusually large and close to one, compared to the other subjects and what has been reported

by Dingwell and Kang (2007).

4.3.2   Walking with the Knee Exoskeleton

In this section, orbital stability analysis has been done on two subjects in three types of experiment: Subjects normal walking (no exoskeleton), subjects walking with the exoskeleton (only on right leg) in passive mode (No active assistant is applied on the subjects, the subjects drive the exoskeleton), and active mode where assistive torque is applied on the subjects by the knee exoskeleton (only on right leg), as explained in chapter 3 The FM values across the gait cycle for all subjects in three mentioned modes are shown in figures 4.6 and 4.7. It must be noted that subject are different from the previous section.

Based on the results shown in figures 4.6 and 4.7, both subjects had orbitally stable walking patterns, in all three modes of experiments, as all FM remained inside the unit circle ($magnitude < 1$). However, the the variation and magnitude of FMs are different for all three modes. The active and passive exoskeleton has obviously affected the orbital stability for the two subjects in different way. In order to get a better statistically understanding of how orbital stability is different in the three experimental modes for each subject, we have derived two measures: the largest max FMs across all poincare sections (101 points across the gait cycle), which is a representation for the most unstable instant during the gait cycle, (Dingwell and Kang, 2007) and also average of the max FMs across the poincare sections and its standard deviation (McAndrew *et al.*, 2011). These measures are driven and compared for the three modes in figure 4.8 and 4.9, respectively.

By comparing the average Max FM across the gait (figure 4.8), it can be seen that the knee motion in passive mode for subject 1 is more unstable in overall across the gait cycle, and applying assistive torque has improved the stability compared to
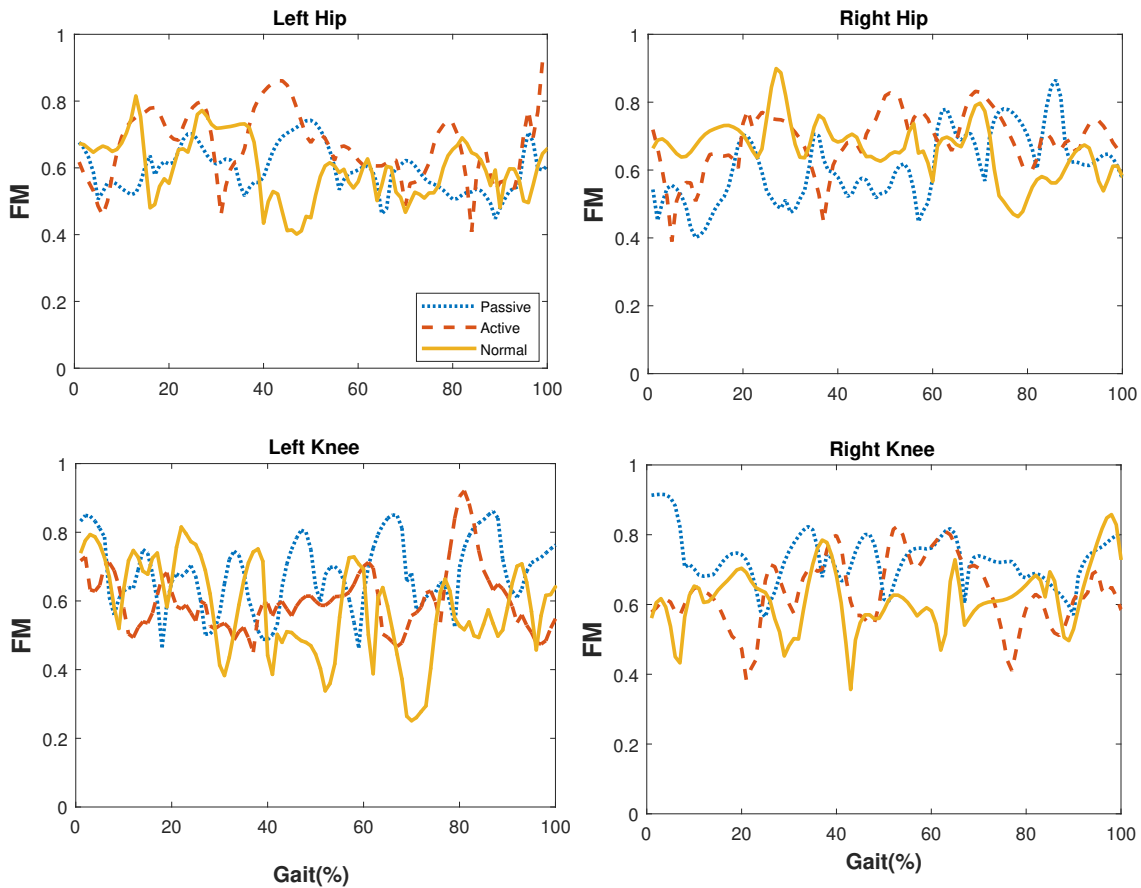
Figure 4.6: Knee and hip joints orbital stability analysis across the gait cycle for the first subject walking on treadmill with the speed of 0.8 m/s, in three modes: Normal level walking (no exoskeleton), Passive walking with the knee exoskeleton, and active assistive torque being applied by the the exoskeleton.

passive walking with the knee exoskeleton. However for subject 1 hip motion, the active assistance from the exoskeleton has increased the average FM across the gait cycle, and is more unstable. Wearing the exoskeleton in passive mode does not seem to have a significant effect on subject 1 hip motion's orbital stability.

For subject 2, figure 4.8 exhibits that for both knee and hip sagital plan motion, walking with active assistance from the knee exoskeleton is the most orbitally sta-
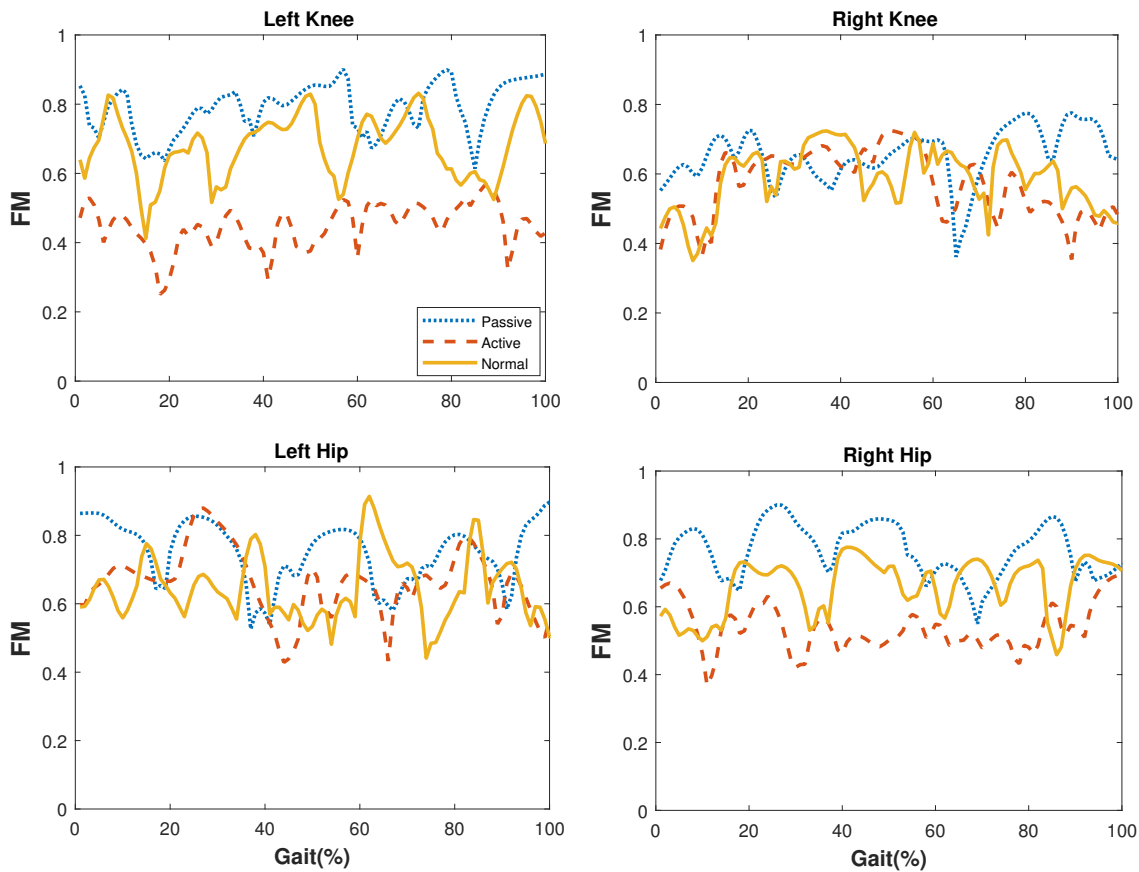
Figure 4.7: Knee and hip joints orbital stability analysis across the gait cycle for the second subject walking on treadmill with the speed of 0.8 m/s, in the same three modes explained in figure 4.6

ble in overall across the gait, while walking with the exoskeleton with no assistance (Passive) is more orbitally unstable, compared to normal and with active assistance walking. By comparing the results of two subjects, it seems that active assistance from the knee exoskeleton has improved and affected the leg motion stability of subject 2, more than subject 1. From the results of both subjects in figure 4.8, It can be concluded that wearing the exoskeleton in passive mode seems to make the walking more unstable compared to normal walking.
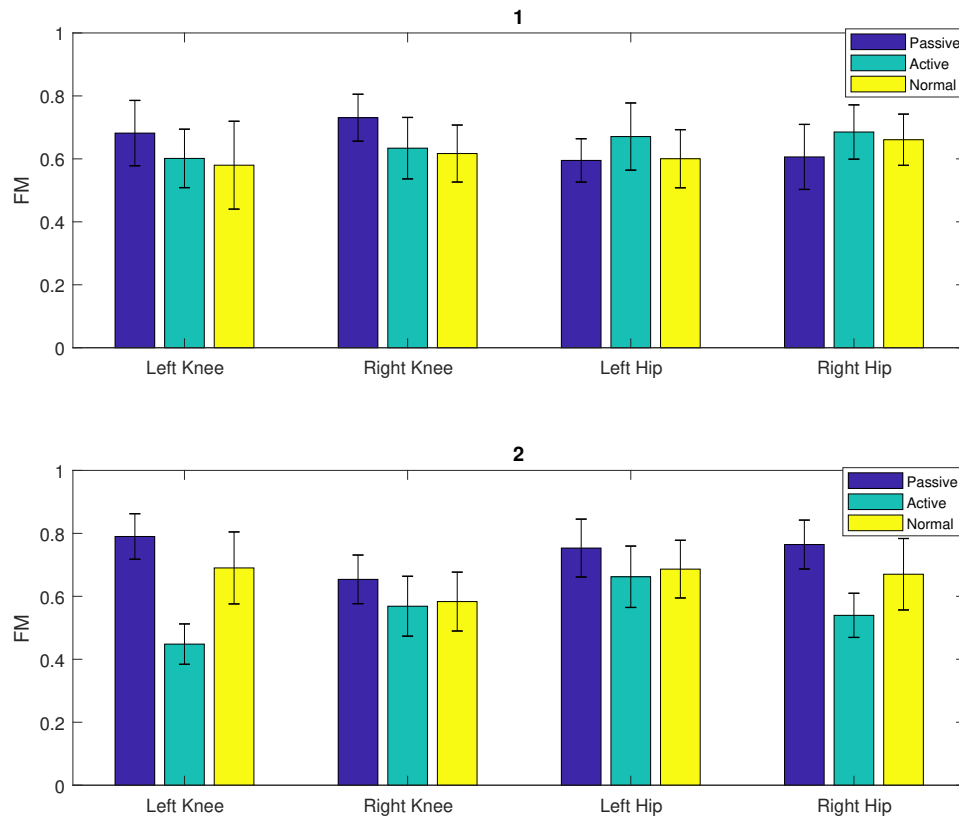
Figure 4.8: Comparison of average and standard deviation of knee and hip joints Max FM across the gait cycle for the two healthy subjects (1 and 2) in three modes of experiment with the knee exoskeleton.

The orbital stability analysis results from figure 4.9, which is comparing the largest knee and hip joints Max FM across the gait cycle for the two subjects, shows that the left knee motion of subject 1 becomes more unstable (close to one) in active mode, compared to the other modes,while the opposite holds true for the right knee. The same trend happens for left and right hip sagital motion of subject 1. It appears that applying assistive torque from the knee exoskeleton to the right knee of subject 1, has different effects on left and right leg joints motion stability, in the sense of the
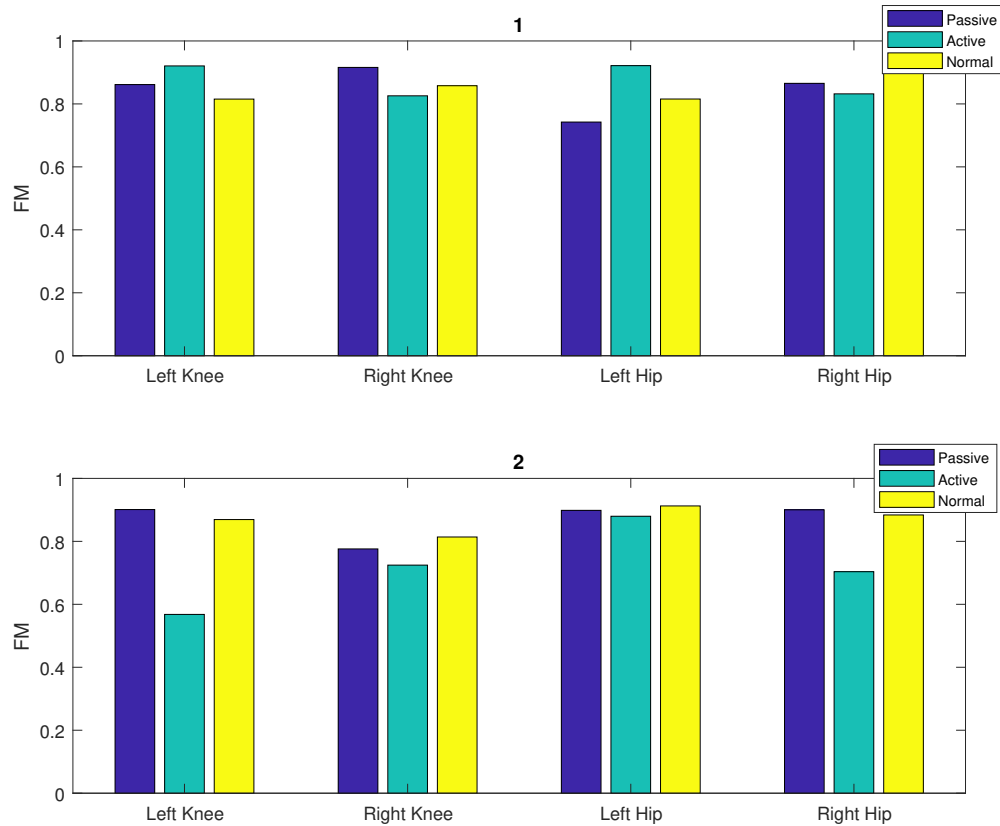
Figure 4.9: Comparison of the largest knee and hip joints Max FM across the gait cycle for the two healthy subjects (1 and 2) in three modes of experiment with the knee exoskeleton.

instant that gets the most unstable. However, the overall average gait stability did not show such trend for this subject.

For subject 2, 4.9 represents the same effect of applying active assistance torque from the exoskeleton, on walking orbital stability, as the largest max FM for subject 2 in active mode for both joint motions, is closer to zero compared to the passive and normal modes. Wearing the exoskeleton in passive mode seems to not have a significant effect on the largest max FM of subject 2, compared to the normal walking. By

comparing the two figures 4.8 and 4.9, it is observed that the difference between the three modes is more significant 4.8, therefore it can be concluded that the knee exoskeleton mostly affects the average max FM of the subjects, rather than the largest one, across the gait cycle. The same trend holds true if the max FM value among the joints be taken into account (figures 4.8 and 4.9), which represents the most unstable motion in the three modes. It can be seen that in figure 4.8 the passive mode for both subjects is the most unstable motion (right knee of subject 1 and left knee for subject 2), while figure 4.9 does not show a significant difference between the most unstable joint motion in the three modes.

4.3.3   Walking with the Robotic Shoe

The same procedure as previous section is done on subjects wearing the robotic shoe, to calculate FM values and quantify gait orbital stability, for three trials: Normal walking, wearing the robotic shoe in passive mode (no external power and actuator) and active mode (controlling the time of exerting push-up torque). More details on data collection and experimental procedure are given in chapter 3.

As it is shown in figure 4.10, the subject is orbitally stable in all three trials as the max FM magnitudes across the gait are less than one. The right ankle orbital stability is clearly affected in passive mode. However for other joint motions, the stability seems to be in the same range in all three modes. This was expected as in chapter 3, it was shown that only the kinematics of the right ankle is significantly different from normal gait pattern while wearing the robotic shoe. It is also must be noted that the right ankle joint motion is more orbitally stable throughout the gait cycle, which could be due to the fact that in active mode the push-up torque is exerted at the right gait phase (toe-off), making the gait cycle less perturbed comparing to
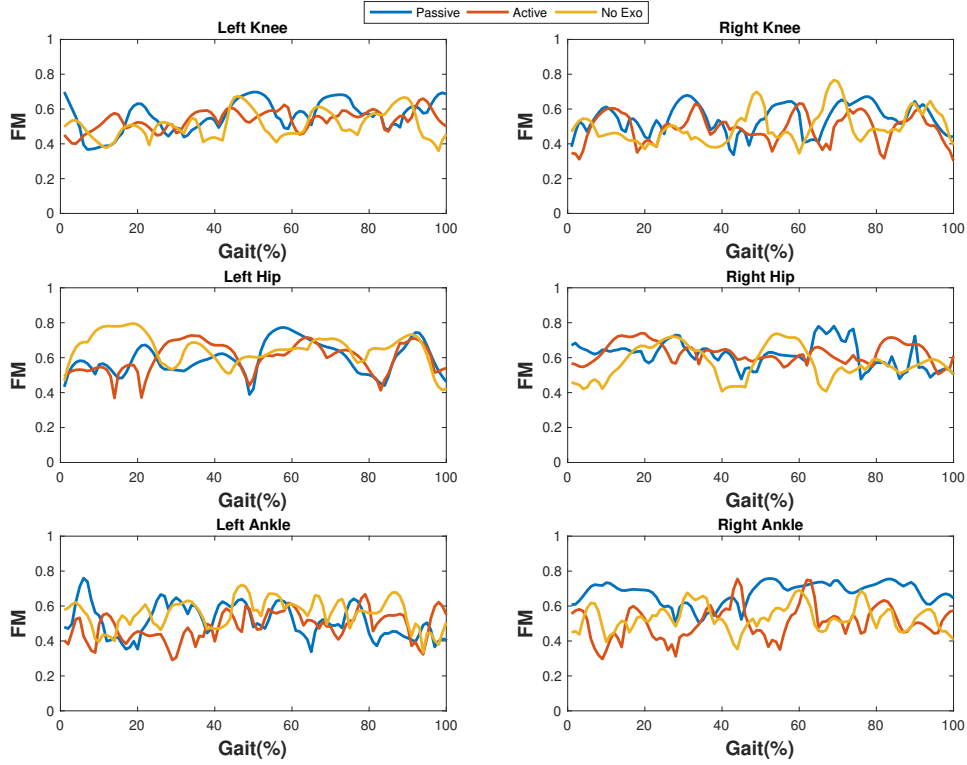
Figure 4.10: Orbital stability analysis for subject 1 wearing the robotic shoe in three modes: Normal (without robotic shoe), passive assistance (no external power) and active assistance.

the passive mode.

The result from figure 4.11 also verifies that the difference between three modes of experiment with robotic shoe for average max FM across the gait, is only significant in right ankle passive mode. The largest max FM does not exhibit such difference.

4.3.4   Walking with Mechanical Perturbations from Treadmill

In this section, the orbital stability analysis has been done on a gait public data set (Moore *et al.*, 2015) that contains both normal walking and mechanically perturbed walking markers time series data. The perturbations are pseudo-random fluctuations
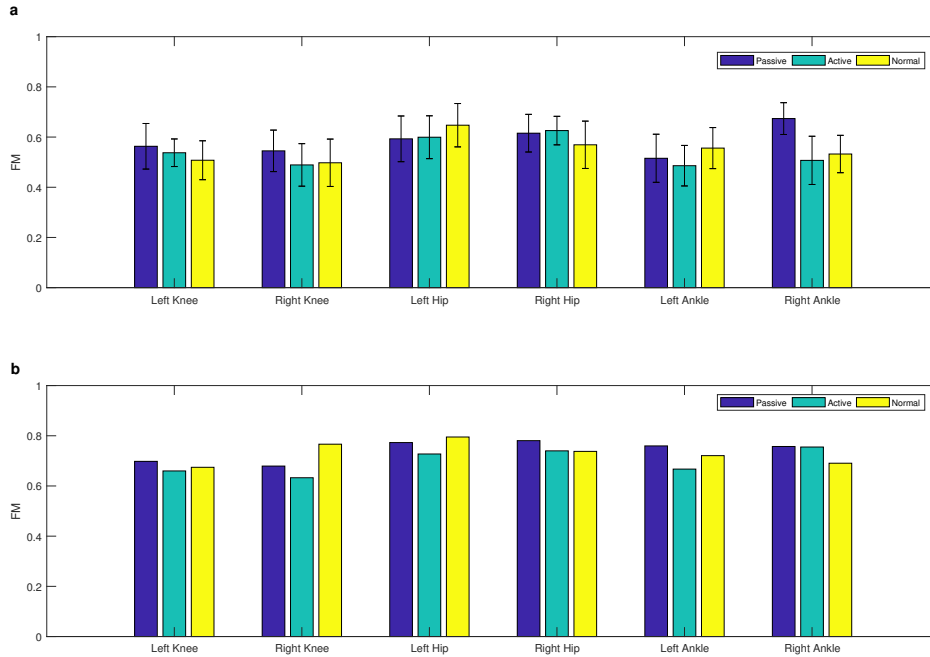
Figure 4.11: Comparison of a) the largest, and b) the average, of knee, hip, and ankle joints Max FM across the gait cycle for subject 1 wearing the robotic shoe in three modes: Normal (without robotic shoe), passive assistance (no external power) and active assistance.

in the speed of the treadmill belt, which not only has been shown to change the joints kinematic and kinetics (Moore *et al.*, 2015), but also give us the sense that it makes the gait less stable and increases the chance of falling. Thus, by doing the orbital stability analysis on this data, it can be seen how these effects are reflected and quantified in orbital stability. This will give us a broader view on using orbital stability as a measure to quantify gait dynamic stability.

Data Collection and processing

The data has been collected by Moore *et al.* (2015) in the following manner: Fifteen healthy subjects including four females and eleven males are asked to walk on a treadmill for about 10 minutes, under unperturbed and perturbed conditions. The data has been collected in the Laboratory for Human Motion and Control at Cleveland State University. 47 markers are used to collect the gait data of subject at 100 Hz sampling rate, using the motion capture system. Each trial includes three main events: Normal walking on treadmill at the specific speed for 1 min, then the longitudinal belt speed perturbation applies to the treadmill and after 8 min of walking under the influence of the perturbations, the second normal walking phase begins which last for 1 min. The longitudinal perturbations applied in the second phase, are pseudo-random belt speed control signals with the mean velocities of the corresponding trial constant velocity. Figure 4.12 shows the fluctuation in treadmill belt speed when these signals are applied.

The raw marker data, time stamps and the instant that each event take places, along with characteristics of subjects and experiment descriptions are provided. These raw data are processed and the lower-limb joints kinematics are extracted by using a modified MATLAB code provided by Moore *et al.* (2015). Then, for each trial the kinematic time series data are categorized in three parts: First normal walking, perturbed walking, and second normal walking.

Results

After exploiting the lower-limb joint angles, the same orbital stability analysis has been done on the data. The analysis has been done on 8 subjects data, as some of the data were erroneous or the reported experiment condition was not ideal. The
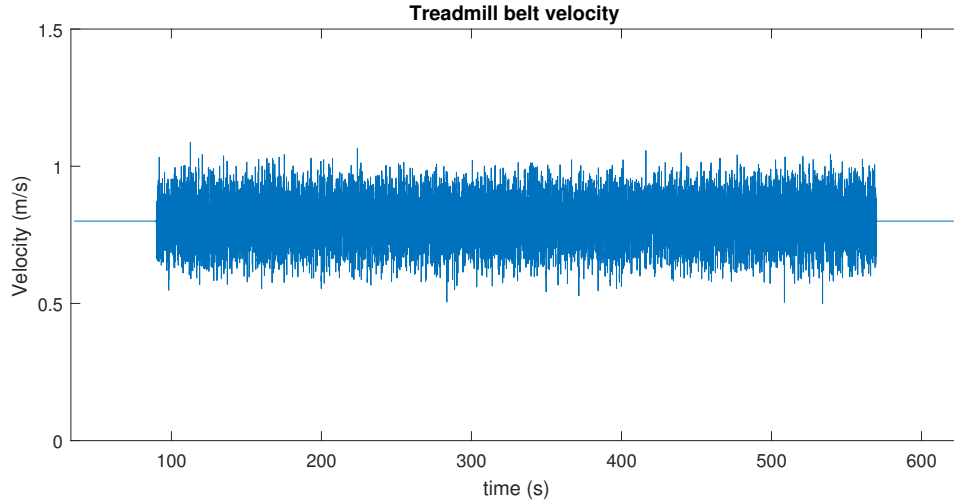
Figure 4.12: The treadmill belt speed for the trials with the velocity of 0.8 m/s. The longitudinal perturbations are applied as pseudo-random belt speed control signals after 1 min of normal walking, and lasts for 8 min, then the second normal walking begins for 1 min.

three phase of each trial; first normal walking, Perturbed walking, and second normal walking has been analyzed separately. 45 strides are considered to calculate the Jacobian and FM values for each phase, since an equal number of strides for all data should be used in order to compare the results. For perturbed walking, the first 45 strides are considered, as they are more likely to be unstable, however, for the steady-state walking pattern (the fixed limit cycle), the average of the whole perturbed walking has been taken into account, as the fixed limit cycle should be a stable walking pattern that might not be the case for only initial parts of perturbed walking, and averaging the the total cycles will give a better stable steady-state walking.

First, the average and largest Max FM of ankle, knee and hip joints across the gait cycle are compared for 8 subjects (figures 4.13 and 4.15, respectively). All subjects exhibited walking orbital stability in all three phases ($|MaxFM| < 1$). It can be

47

observed from the average of FM across the gait cycle that 5 out of 8 subject showed less gait stability (less FM values) in all three joints motion, at the perturbed walking phase, compared to the first and second normal walking, and all subjects had at least one joint motion that was less stable in perturbed walking phase compared to normal walking phases. By comparing 4.13 and 4.15, it can be noted that perturbed walking affects the average gait orbital stability more than the largest max FM (the most unstable instant during the gait cycle), however, by averaging the data of these two figures, it is observed that both measures indicating that perturbed walking has been less orbitally stable, while both normal walking phases has generally same stability.

4.4   Discussion and Conclusion

The main goal of this chapter was to introduce the orbital stability as a measure to analyze the gait dynamic stability, and see how two robotic exoskeletons affects the gait orbital stability. These devices are perturbations to human normal walking, and change its kinematics and kinetics, and consequently might make the gait less stable, more sensitive to external perturbations and, prone to falling. In order to have a better understanding of how external mechanical perturbations affect the gait orbital stability, the same analysis is also done on a public data set where pseudo-random fluctuations are applied on the speed of the treadmill belt, to cause external perturbations to normal walking.

Based on the result of 4.3.2 and 4.3.3 sections, all subjects were orbitally stable with and without the robotic exoskeletons. This was expected, based on the analysis that has been done before in the literature, and the fact that wearing the exoskeletons does not make the subject's gait completely unstable, based on the observations and the corresponding lower-limb gait patterns. However, wearing the exoskeletons, has clearly affected the gait orbital stability.

Figure 4.13: Comparison of the average knee, hip, and ankle joints Max FM across the gait cycle for 8 subjects. N1 is the first normal walking phase, P is the perturbed walking, and N2 is the second normal walking phase. Subject ID number are according to the original published data (Moore *et al.*, 2015)

For the knee exoskeleton, the results showed that the targeted join motion (knee) was more unstable when subjects were wearing it with no assistance (passive), compared to the normal walking (without no device) and with assistance. The knee exoskeleton also affects the orbital stability of the hip joint motion. For subject 2, the same trend as knee joint motion was observed for the hip, meaning the passive mode was the most unstable motion. For subject 1, however, the wearing the exoskeleton in passive mode did not affect the orbital stability significantly, while it was
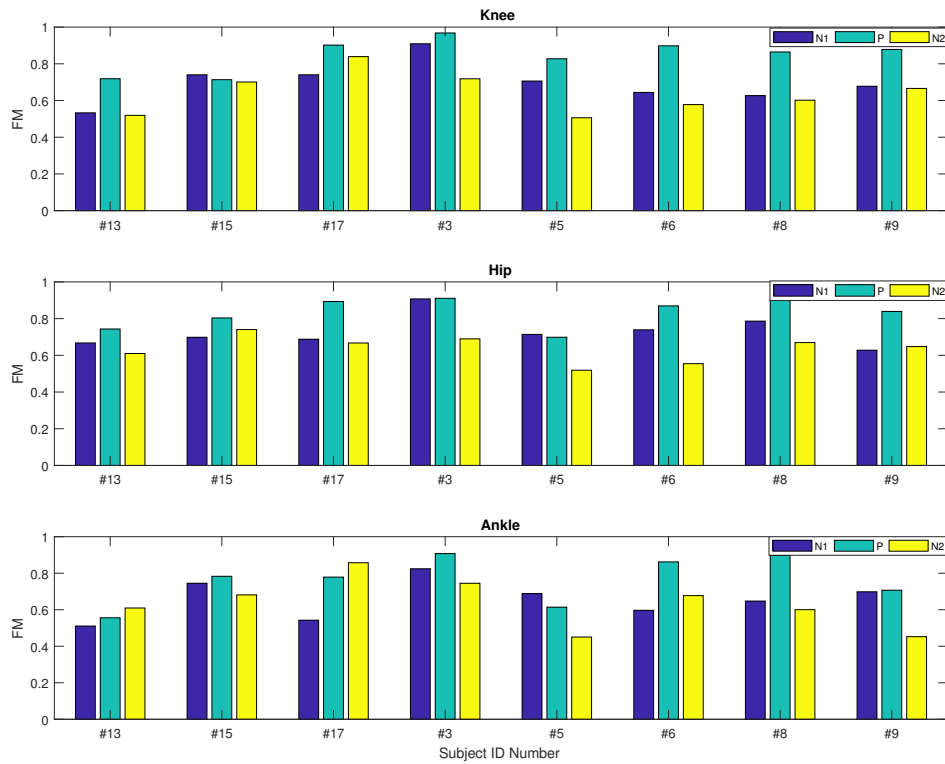
Figure 4.14: Comparison of the largest knee, hip, and ankle joints Max FM across the gait cycle for 8 subjects. N1 is the first normal walking phase, P is the perturbed walking, and N2 is the second normal walking phase. Subject ID number are according to the original published data (Moore *et al.*, 2015)

the active assistance that made the hip sagital motion less stable. In general, the assistance from the exoskeleton, has reduced the max FM across the gait for both hip and knee motion for subject 2, while it had a mixed affect on subject one. People have different gait kinetics and kinematics, which leads to different gait stability, since the assistance was personalized, it is not very surprising that the knee exoskeleton does not have an exact similar impact on subjects gait stability. However the most unstable motion (average of max FM across the gait) among the joints, is passive

50

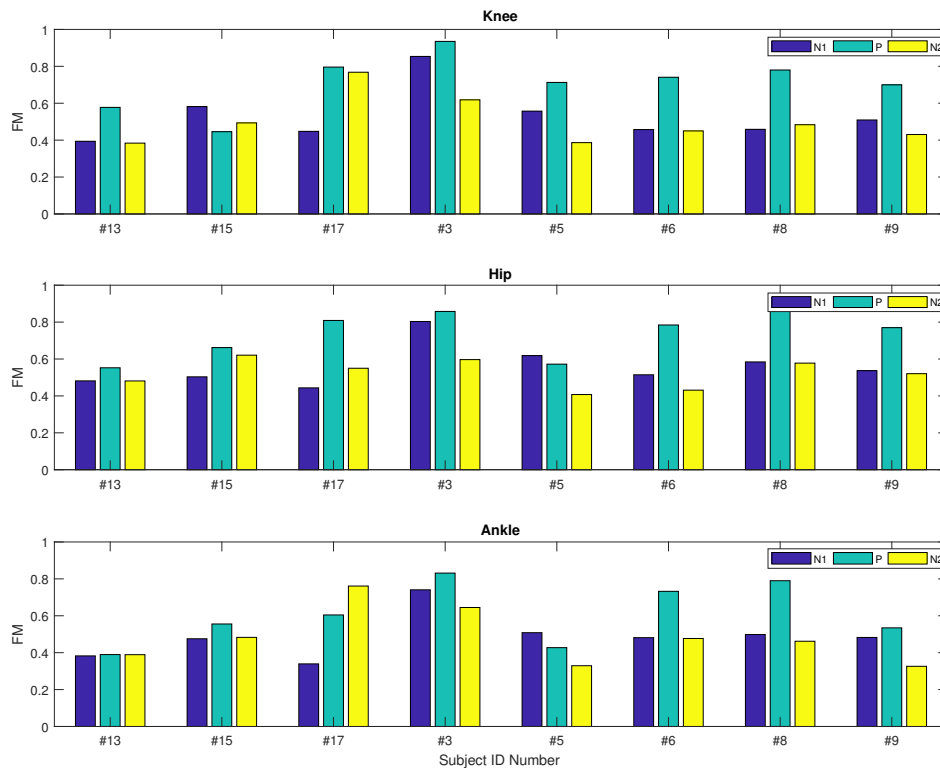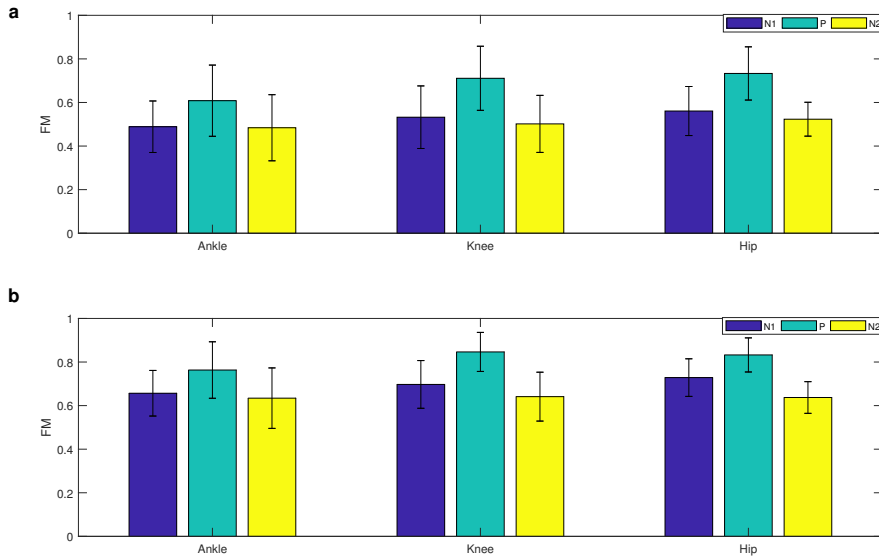Figure 4.15: Comparison of a) the largest, and b) the average, of knee, hip, and ankle joints Max FM across the gait cycle for 8 subjects. N1 is the first normal walking phase, P is the perturbed walking, and N2 is the second normal walking phase. Subject ID number are according to the original published data (Moore *et al.*, 2015)

mode for both subjects. To verify these effects, more experiments in this manner is required.

The results of the same analysis with the robotic shoe showed a significant increase in max FM value across the gait for subject's right ankle (the targeted joint for assistance) sagital plan motion, when wearing the device in passive mode. This was expected as mostly the right ankle motion was affected by the robotic shoe, and also in the passive mode the push-up torque is not released at the right time which makes the gait more perturbed.

By doing the same analysis on a public data set of 8 subjects that contains both normal walking and mechanically perturbed walking (section 4.3.4), the effectiveness

of this analysis on quantifying the impact of external perturbations has been shown. Both statistical measures (average and maximum) of max FM across the gait cycle supported this conclusion by showing a significant increase at perturbed phase, compared to both normal walking phases which were close to each other.

It must be noted that for the robotic shoe and the knee exoskeleton, it was the average of max FM across the gait that showed significant difference in the three modes of experiment, while the largest FM across the gait did not exhibit such obvious difference. For the mechanically perturbed walking data set, both measures exhibited significant increase, therefore it can be concluded that random mechanical perturbation to the walking affects the orbital stability more significantly than the perturbation exerted by the two wearable assistive robots, which is reasonable since the the first perturbation has a clear destabilization effect on walking, while the second one is to assist the human gait and does not necessarily has such effect.

Chapter 5

DISCUSSION AND CONCLUSION

This chapter summarizes the result of this dissertation and discusses its impacts and applications, the challenges and future work.

5.1 Summary of the Work

The design, mechanical mechanism and control of two assistive wearable robots, the knee exoskeleton and the robotic shoe were discussed. The knee exoskeleton provides a personalized knee joint assistive torque during the stance phase, using an automatic impedance tuning algorithm based on the kinematic data from IMUs and ground contact forces from smart shoes, and it was shown that it can reduce the corresponding muscle activity (Tej Chinimilli *et al.*, 2018). The robotic shoe is a light-weighted mechanism that can store the potential energy at heel strike and release it by using an active locking mechanism at the terminal stance phase to provide push-up ankle torque and assist the toe-off. Lower-limb Kinematic time series data were collected for subjects normal walking (without the assistive device), and wearing the assistive devices in the passive and active mode, using the motion capture lab at ASU. The lower-limb joint kinematics were affected by the knee exoskeleton, in both passive and active mode. Both knee and hip sagittal plane motion changed and the motion variability (standard deviation) were significantly different for the three modes of walking. The joint kinematics with the robotic shoe were not greatly affected, except for the targeted joint (right ankle).

There are three main reasons that why the gait stability analysis is done with these wearable assistive robots:

- The physical interaction and assistance from these wearable robots are in nature mechanical perturbation which might affect the gait dynamic stability. It seems essential to quantify their effects and see how gait stability changes by wearing these devices

- It is shown that these devices alter the gait lower-limb joint kinematics such as the range of motion and joint angle patterns, and also increase the variability of motion. These effects are an indication of affecting the gait stability. It is possible that they might have made the users gait more unstable.

- The wearable assistive robots can take gait dynamic stability into account and provide a stable gait, along with the physical assistance. Therefore it is needed to propose a method that can be used as a control design tool to ensure gait stability with these robots.

Orbital stability was chosen to quantify dynamic gait stability, as it is one of the commonly used methods. Orbital stability is defined for a limit cycle system as the tendency of the systems state to return to the periodic limit cycle after perturbations and is quantified through Floquet Multipliers for one discrete cycle to the next. Floquet Multipliers (FM) are the rate of convergence/divergence towards a fixed point or cycle, which are the eigenvalues of the linearization (or Jacobian) of the cycle-to-cycle function. It can be applied to gait as human walking is periodic in nature and shows the limit cycle behavior. This method has been widely used to stabilize the biped robots locomotion and has shown to be able to quantify the effects of perturbation on gait. In addition, the normal walking has been shown to be orbitally stable, while locally unstable.

Gait orbital stability was quantified for walking with two assistive devices in active, passive and normal walking (without the assistive device), using a non-linear

time series analysis. The results with the knee exoskeleton showed that wearing the device in passive mode provides the least orbitally stable gait, across the gait cycle. The active assistance improves the orbital stability for all joint motions of one of the subjects, while having a mixed effect on the other subject, although still decreasing the max FM of all joint motions. The different joints FM patterns for the two subjects can be related to the personalized assistance and the fact that each person's gait has some unique characteristic, and perceive the physical perturbation in different ways.

The stability analysis with the robotic shoe showed that wearing the device with passive assistance makes the gait more unstable, as was expected since in passive mode the assistive torque is not exerted at the right gait phase.

To get more insight on how the mechanical perturbations which potentially make the gait more unstable and increase the risk of falling, could be quantified through orbital stability analysis, a public dataset containing normal and perturbed walking (pseudo-random fluctuations in the speed of the treadmill) of 8 users were used. The results showed a significant increase in FM values for most of the subject in the perturbed walking phase.

5.2   Application and Challenges

As stated before, this work can give a good insight on how two different kinds of assistance can change the gait stability, and provide a control tool design to stabilize walking with the wearable assistive devices. An orbitally stable gait can lead to a dynamic stable gait, as it means the system can respond fast enough to the perturbations and have a robust performance with regard to the steady-state walking pattern that is stable. However, there are still some challenges and drawbacks associated with the methods and results provided.

Using orbital stability as the method to quantify gait dynamic stability is still

debatable. It is argued that human walking is not completely periodic in nature. For example, overground walking shows less periodic behavior compared to treadmill walking, and consequently, it is expected to be less orbitally stable while we do not know how the gait dynamic stability is affected. But it must be noted that Dingwell and Kang (2007) showed overground walking is orbitally stable, and both locally and orbitally less stable compared to treadmill walking, using strain gauge electro-goniometers and accelerometer to analyze both the trunk motion and joint angles. Therefore orbital stability can be used to analyze overground walking, and other less periodic gait activities as well, as long as it can be assumed that they are periodic in nature. Less periodic gait means more deviations from the steady-state walking, however, FM values quantify the rate of those divergences for successive strides, and less periodic behaviour and more variability does not necessarily imply orbital instability as long as each pair of successive strides converge to/don't keep diverging from the steady-state walking pattern.

Orbital stability also does not directly take the effect of variation in stride frequency into account, as each stride is normalized to 101 Poincare sections, to observe the max FM values across the gait cycle. Hak *et al.* (2013) showed that stride frequency affects the medio-lateral margins of stability, however, does not significantly affect the local dynamic stability. Stride frequency has been considered as one of the gait parameters to measure gait variability (Lamoth *et al.*, 2011), while a direct relation between stride frequency variability and risk of falling has not been reported. The effects of change in stride frequency and its variability might be observed in the time-normalized gait pattern, which will influence the FM values.

The orbital stability analysis with wearable assistive robots were done only for two subjects. To verify and better understand the results, more experiments should be performed. There could be possible trends for FM values in the three modes of

the experiment, which can only be extracted by increasing the number of subjects.

Another issue is that FM values are not robust to some factors such as the number of strides, the time delay used to construct the state space, and the experimental conditions. Although it was observed that FM values will still be within a limited range.

In this study, two statistical measures were provided to compare the orbital stability in different modes: the largest and the average of max FM across the gait cycle. It was observed that for some of the joint motions, they did not give the same results, so one should decide which to consider to quantify gait stability, based on their requirement.

5.3   Future Work

To make this work more meaningful and impactful, first, it is essential to perform the same analysis on more subjects with the assistive devices. In addition, Performing local stability analysis to compare with the orbital stability results can lead to a better examination of the gait stability with the assistive devices.

In the end, to complete this work, it is desired to find a way to employ the orbital stability analysis as a design tool to control wearable assistive devices so that they provide dynamic stable gait along with physical assistance.

BIBLIOGRAPHY

Alexander, N. B., "Gait disorders in older adults", Journal of the American Geriatrics Society **44**, 4, 434–451 (1996).

Ali, F. and M. Menzinger, "On the local stability of limit cycles", Chaos: An Interdisciplinary Journal of Nonlinear Science **9**, 2, 348–356 (1999).

Artemiadis, P. K. and H. I. Krebs, "On the potential field-based control of the mitskywalker", in "Robotics and Automation (ICRA), 2011 IEEE International Conference on", pp. 1427–1432 (IEEE, 2011).

Banala, S. K., S. H. Kim, S. K. Agrawal and J. P. Scholz, "Robot assisted gait training with active leg exoskeleton (alex)", IEEE transactions on neural systems and rehabilitation engineering **17**, 1, 2–8 (2009).

Barbareschi, G., R. Richards, M. Thornton, T. Carlson and C. Holloway, "Statically vs dynamically balanced gait: Analysis of a robotic exoskeleton compared with a human", in "Engineering in Medicine and Biology Society (EMBC), 2015 37th Annual International Conference of the IEEE", pp. 6728–6731 (IEEE, 2015).

Berg, W. P., H. M. Alessio, E. M. Mills and C. Tong, "Circumstances and consequences of falls in independent community-dwelling older adults", Age and ageing **26**, 4, 261–268 (1997).

Brach, J. S., S. A. Studenski, S. Perera, J. M. VanSwearingen and A. B. Newman, "Gait variability and the risk of incident mobility disability in community-dwelling older adults", The Journals of Gerontology Series A: Biological Sciences and Medical Sciences **62**, 9, 983–988 (2007).

Bruijn, S. M., "Is stability an unstable concept?: Quantifying dynamic stability of human locomotion", (2010).

Bruijn, S. M., J. H. van Dieën, O. G. Meijer and P. J. Beek, "Statistical precision and sensitivity of measures of dynamic gait stability", Journal of neuroscience methods **178**, 2, 327–333 (2009).

Chelidze, D., "Nonlinear Dynamics Laboratory", `http://egr.uri.edu/nld/software`, [Online; accessed 10-May-2018] (2015).

Chinimilli, P. T., S. Redkar and W. Zhang, "Human activity recognition using inertial measurement units and smart shoes", in "American Control Conference (ACC), 2017", pp. 1462–1467 (IEEE, 2017).

Chinimilli, P. T., S. W. Wachtel, P. Polygerinos and W. Zhang, "Hysteresis compensation for ground contact force measurement with shoe-embedded air pressure sensors", in "ASME 2016 Dynamic Systems and Control Conference", pp. V001T09A006–V001T09A006 (American Society of Mechanical Engineers, 2016).

Chu, A., H. Kazerooni and A. Zoss, "On the biomimetic design of the berkeley lower extremity exoskeleton (bleex)", pp. 4345–4352 (2005).

Colombo, G., M. Joerg, R. Schreier and V. Dietz, "Treadmill training of paraplegic patients using a robotic orthosis", Journal of rehabilitation research and development **37**, 6, 693 (2000).

Deng, W., I. Papavasileiou, Z. Qiao, W. Zhang, K.-Y. Lam and H. Song, "Advances in automation technologies for lower-extremity neurorehabilitation: A review and future challenges", IEEE Reviews in Biomedical Engineering (2018).

Dingwell, J., J. Cusumano, P. Cavanagh and D. Sternad, "Local dynamic stability versus kinematic variability of continuous overground and treadmill walking", Journal of biomechanical engineering **123**, 1, 27–32 (2001).

Dingwell, J., J. Cusumano, D. Sternad and P. Cavanagh, "Slower speeds in patients with diabetic neuropathy lead to improved local dynamic stability of continuous overground walking", Journal of biomechanics **33**, 10, 1269–1277 (2000).

Dingwell, J. B. and J. P. Cusumano, "Nonlinear time series analysis of normal and pathological human walking", Chaos: An Interdisciplinary Journal of Nonlinear Science **10**, 4, 848–863 (2000).

Dingwell, J. B. and H. G. Kang, "Differences between local and orbital dynamic stability during human walking", Journal of biomechanical engineering **129**, 4, 586–593 (2007).

Dingwell, J. B. and L. C. Marin, "Kinematic variability and local dynamic stability of upper body motions when walking at different speeds", Journal of biomechanics **39**, 3, 444–452 (2006).

England, S. A. and K. P. Granata, "The influence of gait speed on local dynamic stability of walking", Gait & posture **25**, 2, 172–178 (2007).

Ferris, D. P., J. M. Czerniecki and B. Hannaford, "An ankle-foot orthosis powered by artificial pneumatic muscles", Journal of applied biomechanics **21**, 2, 189–197 (2005).

Fuller, G. F., "Falls in the elderly.", American family physician **61**, 7, 2159–68 (2000).

Furusho, J., T. Kikuchi, M. Tokuda, T. Kakehashi, K. Ikeda, S. Morimoto, Y. Hashimoto, H. Tomiyama, A. Nakagawa and Y. Akazawa, "Development of shear type compact mr brake for the intelligent ankle-foot orthosis and its control; research and development in nedo for practical application of human support robot", in "Rehabilitation Robotics, 2007. ICORR 2007. IEEE 10th International Conference on", pp. 89–94 (IEEE, 2007).

Garcia, M., A. Chatterjee, A. Ruina and M. Coleman, "The simplest walking model: stability, complexity, and scaling", Journal of biomechanical engineering **120**, 2, 281–288 (1998).

Gates, D. H. and J. B. Dingwell, "Comparison of different state space definitions for local dynamic stability analyses", Journal of biomechanics **42**, 9, 1345–1349 (2009).

Hak, L., H. Houdijk, P. J. Beek and J. H. van Dieën, "Steps to take to enhance gait stability: the effect of stride frequency, stride length, and walking speed on local dynamic stability and margins of stability", PLoS One **8**, 12, e82842 (2013).

Hamed, K. A. and R. D. Gregg, "Decentralized feedback controllers for robust stabilization of periodic orbits of hybrid systems: Application to bipedal walking", IEEE Transactions on Control Systems Technology **25**, 4, 1153–1167 (2017).

Hamed, K. A. and J. W. Grizzle, "Event-based stabilization of periodic orbits for underactuated 3-d bipedal robots with left-right symmetry", IEEE Transactions on Robotics **30**, 2, 365–381 (2014a).

Hamed, K. A. and J. W. Grizzle, "Event-based stabilization of periodic orbits for underactuated 3-d bipedal robots with left-right symmetry", IEEE Transactions on Robotics **30**, 2, 365–381 (2014b).

Hausdorff, J. M., C. Peng, Z. Ladin, J. Y. Wei and A. L. Goldberger, "Is walking a random walk? evidence for long-range correlations in stride interval of human gait", Journal of Applied Physiology **78**, 1, 349–358 (1995).

Herr, H., "Exoskeletons and orthoses: classification, design challenges and future directions", Journal of neuroengineering and rehabilitation **6**, 1, 21 (2009).

Hurmuzlu, Y. and C. Basdogan, "On the measurement of dynamic stability of human locomotion", Journal of biomechanical engineering **116**, 1, 30–36 (1994).

Hurmuzlu, Y., F. GéNot and B. Brogliato, "Modeling, stability and control of biped robotsa general framework", Automatica **40**, 10, 1647–1664 (2004).

Hürmüzlü, Y. and G. D. Moskowitz, "The role of impact in the stability of bipedal locomotion", Dynamics and Stability of Systems **1**, 3, 217–234 (1986).

Karčnik, T., "Stability in legged locomotion", Biological cybernetics **90**, 1, 51–58 (2004).

Kennel, M. B., R. Brown and H. D. Abarbanel, "Determining embedding dimension for phase-space reconstruction using a geometrical construction", Physical review A **45**, 6, 3403 (1992).

Kong, K., J. Bae and M. Tomizuka, "A compact rotary series elastic actuator for human assistive systems", IEEE/ASME transactions on mechatronics **17**, 2, 288–297 (2012).

Lamoth, C. J., F. J. van Deudekom, J. P. van Campen, B. A. Appels, O. J. de Vries and M. Pijnappels, "Gait stability and variability measures show effects of impaired cognition and dual tasking in frail people", Journal of neuroengineering and rehabilitation **8**, 1, 2 (2011).

Maki, B. E., "Gait changes in older adults: predictors of falls or indicators of fear?", Journal of the American geriatrics society **45**, 3, 313–320 (1997).

McAndrew, P. M., J. M. Wilken and J. B. Dingwell, "Dynamic stability of human walking in visually and mechanically destabilizing environments", Journal of biomechanics **44**, 4, 644–649 (2011).

Moore, J. K., S. K. Hnat and A. J. van den Bogert, "An elaborate data set on human gait and the effect of mechanical perturbations", PeerJ **3**, e918 (2015).

Nayfeh, A. H. and B. Balachandran, *Applied nonlinear dynamics: analytical, computational and experimental methods* (John Wiley & Sons, 2008).

Perry, J., J. R. Davids *et al.*, "Gait analysis: normal and pathological function", Journal of Pediatric Orthopaedics **12**, 6, 815 (1992).

Perry, M., "Science and innovation strategic policy plans for the 2020s (eu, au, uk): Will they prepare us for the world in 2050?", Applied Economics and Finance **2**, 3, 76–84 (2015).

Richardson, J. K. and E. A. Hurvitz, "Peripheral neuropathy: a true risk factor for falls", The Journals of Gerontology Series A: Biological Sciences and Medical Sciences **50**, 4, M211–M215 (1995).

Shorter, K. A., J. Xia, E. T. Hsiao-Wecksler, W. K. Durfee and G. F. Kogler, "Technologies for powered ankle-foot orthotic systems: Possibilities and challenges", IEEE/ASME Transactions on mechatronics **18**, 1, 337–347 (2013).

Takens, F., "Detecting strange attractors in turbulence", in "Dynamical systems and turbulence, Warwick 1980", pp. 366–381 (Springer, 1981).

Tej Chinimilli, P., Q. Zhi, S. M. R. Sorkhabadi, V. Jhawar, I. H. Fong and W. Zhang, "Automatic virtual impedance adaptation of a knee exoskeleton for personalized walking assistance (to be submitted)", (2018).

Varol, H. A., F. Sup and M. Goldfarb, "Multiclass real-time intent recognition of a powered lower limb prosthesis", IEEE Transactions on Biomedical Engineering **57**, 3, 542–551 (2010).

Veneman, J. F., R. Kruidhof, E. E. Hekman, R. Ekkelenkamp, E. H. Van Asseldonk and H. Van Der Kooij, "Design and evaluation of the lopes exoskeleton robot for interactive gait rehabilitation", IEEE Transactions on Neural Systems and Rehabilitation Engineering **15**, 3, 379–386 (2007).

Vukobratovic, M., B. Borovac, D. Surla and D. Stokic, *Biped locomotion: dynamics, stability, control and application*, vol. 7 (Springer Science & Business Media, 2012).